*Journal of Extracellular Vesicles*

RESEARCH ARTICLE OPEN ACCESS

# Comprehensive Phenotyping of Extracellular Vesicles in Plasma of Healthy Humans – Insights Into Cellular Origin and Biological Variation

Marija Holcar[1] | Ivica Marić[2,3] | Tobias Tertel[4] | Katja Goričar[1] | Urška Čegovnik Primožič[5] | Darko Černe[5] | Bernd Giebel[4] | Metka Lenassi[1]

[1]Institute of Biochemistry and Molecular Genetics, Faculty of Medicine, University of Ljubljana, Ljubljana, Slovenia | [2]Department of Immunohaematology, Blood Transfusion Centre of Slovenia, Ljubljana, Slovenia | [3]Faculty of Medicine, University of Ljubljana, Ljubljana, Slovenia | [4]Institute for Transfusion Medicine, University Hospital Essen, University of Duisburg-Essen, Essen, Germany | [5]Clinical Institute for Clinical Chemistry and Biochemistry, University Medical Centre Ljubljana, Ljubljana, Slovenia

**Correspondence:** Metka Lenassi (metka.lenassi@mf.uni-lj.si)

**Received:** 4 July 2024 | **Revised:** 21 December 2024 | **Accepted:** 2 January 2025

**Funding:** This work was supported by the Slovenian Research and Innovation Agency (ARIS) under Grant P1-170 and the Blood Transfusion Centre of Slovenia under Grant 5966.

**Keywords:** blood | biological variation | extracellular vesicles | healthy humans | plasma

## ABSTRACT

Despite immense interest in biomarker applications of extracellular vesicles (EVs) from blood, our understanding of circulating EVs under physiological conditions in healthy humans remains limited. Using imaging and multiplex bead-based flow cytometry, we comprehensively quantified circulating EVs with respect to their cellular origin in a large cohort of healthy blood donors. We assessed coefficients of variations to characterize their biological variation and explored demographic, clinical, and lifestyle factors contributing to observed variation. Cell-specific circulating EV subsets show a wide range of concentrations that do not correlate with cell-of-origin concentrations in blood, suggesting steady-state EV subset concentrations are regulated by complex mechanisms, which differ even for EV subsets from the same cell type. Interestingly, tetraspanin+ circulating EVs largely originate from platelets and to a lesser extent from lymphocytes. Principal component analysis (PCA) and association analyses demonstrate high biological inter-individual variation in circulating EVs across healthy humans, which are only partly explained by the influence of sex, menopausal status, age and smoking on specific circulating EV and/or tetraspanin+ circulating EV subsets. No global influence of the explored subject's factors on circulating EVs was detected. Our findings provide the first comprehensive, quantitative data towards the cell-origin atlas of plasma EVs, with important implications in the clinical use of EVs as biomarkers.

## 1 | Introduction

Plasma, the liquid part of the blood, is the predominant source for extracellular vesicle (EVs) biomarker, therapeutic, and functional studies (Royo et al. 2020; Beetler et al. 2023). Despite huge interest, we have limited knowledge of the circulating EVs under physiological conditions in healthy humans. Their total concentration was estimated from $10^6$ EVs/mL with flow cytometry to up to $10^{13}$ EVs/mL with nanoparticle tracking analysis (NTA) (Johnsen et al. 2019). With respect to the cellular source of

Marija Holcar and Ivica Marić contributed equally to this study.

circulating EVs, platelet-derived and erythrocyte-derived EVs are in the range of $10^7$ EVs/mL, while quantification of EVs derived from leukocyte subsets in plasma is mostly missing (Arraud et al. 2014; Bettin et al. 2022; Kumar et al. 2024). Digital quantification based on the long RNA profiles estimated that 99.8% of circulating EVs originate from haematopoietic cells, mostly from platelets, B cells, and CD4 T cells (Li et al. 2020), but the extent to which RNA is packed into EVs is controversial (Tosar, Witwer, and Cayota 2021; Mosbach et al. 2021). Several recent proteomics studies have provided comprehensive protein composition of circulating EVs in healthy humans (Rai et al. 2024; Vallejo et al. 2023; Muraoka et al. 2022), but there is a lack of quantification at the single vesicle level. Thus there is a key need for comprehensive single vesicle quantification of circulating EVs in healthy humans.

Importantly, the relationship between concentrations of specific blood cells and concentrations of circulating EVs is unclear. At any time, the steady-state concentration of circulating EVs is the equilibrium of EV secretion and uptake, but direct measurements in human plasma are missing. To address this, Auber and Svenningsen integrated available data on circulating EVs and blood cells and estimated the highest EV secretion rates for monocytes and the lowest for erythrocytes, with platelets in the middle (Auber and Svenningsen 2022). EV uptake studies in animal models identified macrophages and endothelial cells in mice, and B cells in macaques, as largely responsible for EV clearance from blood in a few minutes to a few hours (Driedonks et al. 2022; Eitan et al. 2017; Loconte et al. 2023; Matsumoto et al. 2021). A more direct approach to studying the relationship between specific blood cell concentrations and levels of circulating EVs, with respect to their cell of origin, is to perform quantification and association studies on a large healthy human cohort.

Another fairly neglected aspect of circulating EVs is intrinsic biological variation across healthy humans. Understanding biological variation is fundamental for circulating EVs' clinical application, especially for interpretation of EV-based disease biomarker readouts. The biological variation of commonly examined plasma quantities is widely documented, most showing higher inter-individual than intra-individual variation (Aziz et al. 2019; Widjaja et al. 1999). To improve clinical decisions, reference intervals for most haematological quantities are also stratified by sex and/or age (L. Van Pelt et al. 2022; Ozarda, Higgins, and Adeli 2019). In the case of circulating EVs, current studies imply the influence of age, sex, smoking and physical activity. Individual studies on small circulating EVs in healthy humans showed decreased plasma extracellular particle concentration with advancing age (Eitan et al. 2017), increased levels of tetraspanin+ circulating EVs during cycling exercise (Brahmer et al. 2019) and changes in tetraspanin+ circulating EVs protein profiles in smokers, depending on sex (Bæk, Varming, and Jørgensen 2016). Flow cytometric studies of large circulating EVs showed higher levels of EVs derived from platelets and endothelial cells in females compared to males (Gustafson et al. 2015), and the influence of age, sex and smoking status on specific EV subsets (Enjeti et al. 2017). So far, there are no comprehensive studies of circulating EVs biological variation in large healthy human cohorts, and the impact of demographic, clinical, and lifestyle factors on the latter.

The aim of this study was to improve the understanding of circulating EVs under physiological conditions by comprehensively quantifying circulating EVs with respect to their cell of origin in healthy humans, determining their biological variation and exploring demographic, clinical, and lifestyle factors contributing to the observed variation. To this end, we performed surface protein phenotyping of EVs in plasma and in isolated tetraspanin+ circulating EVs in a large well-characterized cohort of blood donors, using imaging and multiplex bead-based flow cytometry. We calculated coefficients of variation (CV) for concentrations of circulating EV subsets and marker expression levels of tetraspanin+ circulating EVs to characterize biological variation and conducted association analyses to explore the influence of demographic, clinical, and lifestyle factors on the latter.

## 2 | Materials and Methods

### 2.1 | Study Design and Subjects

We performed a cross-sectional study that included 208 adults who donated blood at the Blood Transfusion Centre of Slovenia between July 27 and 23 November 2020. The study design is represented in Figure 1. The study subjects were equally distributed between sexes (M/F) and four age groups (18–29 years; 30–44 years; 45–54 years; 55–64 years). All subjects were Caucasians and had eaten a non-fatty meal prior to blood donation according to the general guidelines for blood donation. Only individuals who exhibited no signs of illness according to the Slovenian blood donation eligibility requirements, which are aligned with The European Directorate for the Quality of Medicines & HealthCare guidelines (EDQM 2023) and were not taking any medications or hormonal contraception at the time, were included in the study. The eligibility of study subjects was further determined through a comprehensive medical interview and examination always conducted by the same physician. Collected fully anonymized data included the subjects' demographics (age, sex), clinical (body temperature, height, weight, body mass index (BMI), blood pressure, blood pulse, menopause status), and lifestyle (exercise regimen, time since last exercise, smoking status) factors. Written informed consent was obtained from all patients. The study was approved by the Slovenian National Ethics Committee (0120-209/2020/3) and conducted in accordance with the Declaration of Helsinki.

### 2.2 | Blood Collection and Routine Laboratory Analysis

Blood collection was performed during routine blood donation from a satellite bag into serum (5 mL, BD Vacutainer, UK) and plasma (anticoagulant ethylenediaminetetraacetic acid; EDTA K3/7.5 mL, S-Monovette, Sarstedt, Germany) vacutainer tubes. All blood donations occurred between 7 and 11 AM from a cubital vein, using a butterfly system with a 16G needle and a tourniquet. Whole blood was then routinely analysed to determine complete blood count and exclude common infections (HIV, HBV, HCV, and syphilis).

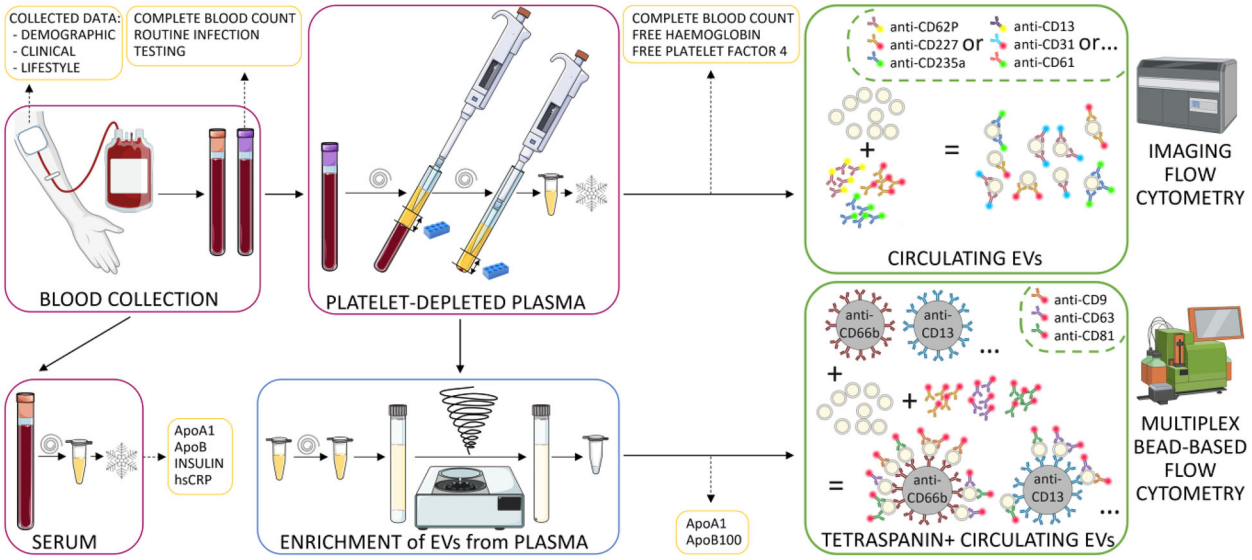


**FIGURE 1** | Schematic representation of the study workflow. ApoA1—apolipoprotein A1; ApoB—apolipoprotein B; hsCRP—highly sensitive measurement of C-reactive protein. Image created by Biorender.com and Smart.servier.com.

### 2.3 | Platelet-Depleted Plasma and Serum Preparation

Serum was prepared by leaving whole blood to coagulate for 30 min at room temperature, followed by centrifugation for 10 min at 2000 × *g* (Eppendorf Centrifuge 5702, Hamburg, Germany). Serum was then aliquoted into 1 mL portions and frozen at −80°C until further analysis. Plasma was prepared according to the guidelines of the International Society for Thrombosis and Haemostasis protocol for generating platelet-depleted plasma (Lacroix et al. 2012; Nieuwland and Siljander 2024) as follows: after collection, blood was mixed with an anticoagulant by gently turning the tube six times and then placed in an upright position in the tube rack. Next, two 15-min consecutive centrifugations at room temperature and 2500 × *g* were performed without a brake (Eppendorf Centrifuge 5804, Hamburg, Germany). After the first centrifugation, plasma was transferred into a fresh tube. Special care was taken to leave 1 cm of plasma above the sedimented cells after both centrifugation steps. Complete blood count measurements were repeated in plasma (Cell-Dyn Ruby Haematology Analyzer, Abbott, Chicago, IL, USA), then plasma was aliquoted into 1-mL portions and frozen at −80°C until further analysis. Plasma and serum preparations were performed in the same facility as blood donations, always by the same person, and aliquoted and frozen within 4 h of blood donation. All information regarding plasma and serum preparation is reported also as the MIBlood-EV report.

### 2.4 | Measurement of Lipoproteins, C-Reactive Protein (CRP), and Insulin

The lipid profile, highly sensitive measurements of concentrations of C-reactive protein (hsCRP), and insulin were measured in the defrosted serum. The lipid profile was determined by routine nephelometric measurements of apolipoprotein A1 (ApoA1) and apolipoprotein B (ApoB) concentrations using a routine analyser (Atellica NEPH 630, Siemens, Germany) and commercial reagents (N AS APOAI, N AS APOB, Siemens, Germany).

To measure the concentrations of CRP and insulin, we used commercially available ELISA kits: hs-CRP Human C-Reactive Protein ELISA Kit (#RAB0096, Sigma-Aldrich, Germany) and Mercodia Insulin ELISA (#10-1113-01, Mercodia, Sweden). Both ELISAs were performed in duplicates, according to the manufacturer's instructions.

### 2.5 | Measurement of Free Haemoglobin and Platelet Factor 4

Free plasma haemoglobin and platelet factor 4 (PF4) concentrations were measured in defrosted plasma. Free haemoglobin was measured spectrophotometrically by measuring $A_{380}$, $A_{415}$, and $A_{450}$. Concentration was calculated according to the Harboe method with Allen correction: $Hb(g/L) = (167.2 \times A_{415} - 83.6 \times A_{380} - 83.6 \times A_{450}) \times (1/1000) \times$ dilution in $dH_20$ (Han, Serrano, and Devine 2010). Samples of plasma with a haemoglobin concentration greater than 0.5 g/L were considered haemolysis (Han, Serrano, and Devine 2010). The concentration of PF4 was measured using a commercially available ELISA kit (#EHPF4, Invitrogen, USA) in duplicate, according to the manufacturer's instructions.

### 2.6 | Imaging Flow Cytometry Analysis

Following defrosting, aliquots of plasma samples were centrifuged at 10,000 × *g* for 10 min at 4°C to remove larger particles and cryoprecipitates. The supernatant was carefully transferred to new containers to avoid contamination. For antibody staining, aliquots of 10 µL plasma were incubated with fluorescently labelled antibodies targeting EV-surface proteins. Up to four antibodies were used per measurement and a combination was selected that resulted in a maximum of one double staining on

one EV. The cellular origin of chosen markers (Table S1) was determined based on established markers recognized in flow cytometry as indicative of specific cells. ("CD Marker Handbook Human and Mouse" 2016). A detailed description of the amounts used and allocation of antibodies to assays is given in Tables S2 and S3. The antibodies were diluted in 10 µL of PBS and incubated with the plasma aliquots at room temperature for 1 h to allow for optimal binding. Following incubation, the samples were diluted to a final volume of 100 µL with PBS for analysis (10× dilution). In adherence to the MIFlowCyt-EV criteria for EV analysis (Welsh et al. 2020), we included various controls in our experimental design. These included buffer-only controls, buffer plus antibody controls, fluorochrome-conjugated isotype controls, and detergent lysis controls using 2% NP-40 in PBS. The checklist for MIFlowCyt-EV can be found in the supplement.

All stained samples were analysed using an AMNIS ImageStreamX Mark II Flow Cytometer (AMNIS/Luminex, Seattle, WA, USA) equipped with an autosampler for U-bottom 96-well plates (Corning Falcon, cat 353077) after molecules of equivalent soluble fluorophores (MESF) calibration for fluorescence quantification, as described previously (Tertel, Görgens, and Giebel 2020). The results can be found in Figure S1. The cytometer settings were adjusted to an acquisition time of 5 min per well, utilizing a 60× magnification and a low flow rate (0.3795 ± 0.0003 µL/min). This setup allowed for high-resolution imaging of EVs without the need for bead removal, as per our previous protocols (Görgens et al. 2019; Tertel et al 2020). The laser and filter configuration are given in Table S4 and the compensation matrix in Table S5. Events were gated using a side scatter (SSC) threshold of 10,000 arbitrary units, selecting events corresponding to polystyrene beads smaller than 200 nm in size, thereby filtering out events corresponding to larger particles (vesicles, cellular debris, or aggregates in nature). Fluorescence intensity threshold of 300 was set after MESF calibration, ensuring that only events with detectable surface marker expression (e.g., CD9, CD63, CD81) above background noise were considered for EV subset concentration calculations. MESF calibration enables equal application of the same threshold to all fluorophores, and consequently to all studied protein markers. Events characterized by low side scatter (< 10,000) and a fluorescent intensity higher than 300 were considered for EV concentration calculations, as detailed in our previous studies (Tertel, Görgens, and Giebel 2020).

The imaging flow cytometry dataset supporting this study is available upon request, with the understanding that it is substantial in size and comprises large number of fcs files.

## 2.7 | Enrichment of EVs With Sucrose Cushion Ultracentrifugation (sUC)

EVs were enriched from plasma following our previously established protocol (Holcar et al. 2020). Briefly, upon defrosting 1 mL aliquots of plasma on ice, the samples were centrifuged at 10,000 × *g* for 20 min at 4°C to remove larger particles and cryoprecipitates. Subsequently, 900 µL of supernatant was diluted with 8.5 mL of particle-free Dulbecco's phosphate-buffered saline (DPBS, Sigma-Aldrich, USA) and carefully layered over 2 mL of 20% sucrose (Merck Millipore, USA) in polypropylene tubes (Beckman Coulter, USA). The samples were ultracentrifuged at 100,000 × *g* for 135 min at 4°C (MLA-55 rotor, Beckman Coulter, USA). After removal of the supernatant, the pellet containing enriched EVs was resuspended in 60 µL of DPBS, aliquoted into 20 µL samples, and stored at −80°C. All EV enrichments were performed by the same person in the same laboratory within 2 months.

## 2.8 | Quantification of Extracellular Particles (EP) by NTA

NTA was used to quantify the size and concentration of EP in the samples of enriched EVs. Samples were diluted in DPBS to $1 \times 10^7$–$10^9$ EPs/mL and examined using a NanoSight NS300 (NanoSight Ltd., UK) equipped with a 488 nm blue laser and automated sample assistant for automated loading of the samples into the instrument. Duplicate samples were pipetted into 96-well plates and five 60-s-long videos were captured for each replicate at camera level 15. After visual inspection, videos with visible artefacts were removed and three videos from each replicate were chosen for analysis. To correct for potential inter-plate variation in NTA measurements, an internal reference sample of enriched EVs was added in duplicates to each plate and used for the normalization of analysed EV samples.

The reference sample of enriched EVs was prepared in-house from a large batch of conditioned media collected from HEK293 cells. The EVs were enriched by differential ultracentrifugation (300 × *g*/20 min/room temperature/max brake; 10.000 × *g*/30 min/4°C/max brake; 100.000 × *g*/110 min/4°C/max brake; washing by repeating the last step in fresh dPBS), aliquoted, and frozen at −80°C for future use. For each NTA measurement, a fresh aliquot was defrosted to ensure sample consistency.

Raw laser scattering and particle movement data were analysed using NTA software (version 3.3; NanoSight Ltd., UK). Automatic settings were selected for the maximal track length, minimum expected particle size and blur, minimum track length was set to 10, detection threshold to 5, and sample viscosity to the corresponding viscosity for water and temperature to 25°C. The output data are presented as EP size (modal hydrodynamic diameter in nm) and EP concentration (number of EPs enriched from 1 mL of plasma in particles/mL of plasma). The analytical coefficient of variation (% CV) was calculated from the variations in the six measurements of each sample. All analyses were performed by the same person in the same laboratory within 8 months after EV enrichment from plasma.

## 2.9 | Multiplex Bead-Based Flow Cytometry Analysis

For semi-quantitative analysis of 37 different surface protein markers, which co-express with at least one of the tetraspanins of enriched circulating EVs, we used a commercial multiplex bead-based flow cytometry kit (MACSPlex Exosome Kit, human,

Miltenyi Biotec, Germany) according to the manufacturer's instructions and analysed the samples with MACSQuant Analyzer 10 (Miltenyi Biotec, Germany). In short, $1 \times 10^9$ (according to NTA analysis) of enriched EPs were incubated overnight in the dark at room temperature with a mix of polystyrene capturing beads (each bead coated with one type of specific antibodies) for the detection of 37 EV surface markers and 2 isotype controls. After the incubation, a cocktail of detection antibodies against tetraspanins (mix of anti-CD9, anti-CD63, and anti-CD81 antibodies), all conjugated with APC, was added, and median fluorescence intensity (MFI) was measured (MACSQuant Analyser 10, Miltenyi Biotec, Germany). As a control, MACSPlex Buffer alone was incubated with beads and detection antibodies. The results of MFI measurements were normalized according to the manufacturer's instructions. First, the background was corrected by subtracting the MFI of the buffer-only sample. Next, the MFIs of each sample were normalized by their respective normalization factors, calculated by dividing the mean MFI of CD9, CD63, and CD81 signal of the respective sample with the mean MFI of CD9, CD63, and CD81 signal of all samples. When referring to measured MFI levels, we introduced the term 'marker expression' level, as MFIs reflect both changes in concentration of specific tetraspanin+ circulating EV subset and changes in expression of measured protein markers on those EV subsets.

### 2.10 | Statistical Analysis

Statistical analyses were performed using IBM SPSS Statistics, version 27.0 (IBM Corporation, Armonk, NY, USA) and GraphPad Prism, version 9.4.0 (GraphPad Software, La Jolla, CA, USA).

Continuous variables were described as the median and interquartile range (25%–75%), whereas categorical variables were described using frequencies. Non-parametric Kruskal–Wallis and Mann–Whitney tests were used to compare the distribution of continuous variables between different subject groups. Spearman's rho correlation coefficient ($\rho$) was used to assess correlations between continuous variables. For significant associations, $\rho$ between 0.3 and 0.6 or −0.3 and −0.6 was considered fair, and above 0.6 or below −0.6 was moderate or strong (Akoglu 2018). All statistical tests were two-sided, and the level of significance was generally set to 0.05, except for analyses of multiple EV subsets or surface markers on tetraspanin+ EVs, where Bonferroni correction was considered. As 25 or 23 EV subsets or EV-surface proteins were evaluated using imaging or multiplex bead-based FC, respectively, $p$ values below 0.002 were considered statistically significant in this part of the analysis. % CV was calculated as (standard deviation/sample mean) × 100 to measure the relative dispersion of data points in a data series around the mean. We used principal component analysis (PCA) for dimensionality reduction and data visualization when analysing the influence and co-dependence of 25 EV subset concentrations or 23 EV-surface protein expressions. PC1 and PC2 represent the first and second principal components, respectively, which are linear combinations of the original variables that capture the maximum variance in the data. Loadings refer to the weights assigned to each original variable in the calculation of principal components, indicating their contribution to the variance observed in the data.

## 3 | Results

### 3.1 | Characterization of Study Subjects Supports Apparent Health of Recruited Adult Blood Donors

To gain insight into the circulating EVs under physiological conditions in the plasma of healthy humans, we recruited 208 adult blood donors who satisfied all general requirements for Slovenian blood donation eligibility (including the absence of any sign of illness) and were not taking any medications or hormonal contraception at the time. They all tested negative for HIV, HBV, HCV, and syphilis infections and had normal CRP levels, measured at high sensitivity by ELISA, implying an absence of inflammation or infection. Study subjects were further characterized for demographic, clinical, and lifestyle factors by in-depth interviews, examinations and routine blood tests (Table 1). Study subjects matched by sex and age (18–65 years, median age 44.5 years) had a median BMI representative of Slovenian population (25.6 [25%–75%: 22.8–28.1] kg/cm$^2$) (Jakše, Godnov, and Pinter 2022). Their body temperature, blood pressure, and blood pulse were inside respective reference ranges. The study subjects' metabolism balance was described by serum lipoproteins (ApoA1 and ApoB) and insulin concentrations, all measured by ELISA. No impact of lipoprotein or insulin concentrations on any of the EV characteristics studied here was observed (Table S6).

Twenty-nine percent of study subjects were active smokers (30 males and 30 females). All study subjects reported regular exercise, with 16.8% describing it as intensive, however, for most (76%) the last exercise happened more than 48 h before the blood draw (Table 1). As expected, the median erythrocyte concentration in the blood of study subjects was the highest of all measured cell types at $4.91 \times 10^9$/mL, with platelet and leukocyte median concentrations 22 times and 790 times lower, respectively. Neutrophils, the most numerous granulocytes, represented 56% of leukocytes in the blood, while lymphocytes and monocytes represented 33% and 8%, respectively (Table S7). This distribution aligns with the typical composition of blood in apparently healthy adults (Troussard et al. 2014).

To ensure consistency and minimize pre-analytical variables, plasma was prepared within 4 h of blood draw, by the same individual at the same facility, following the standard protocol outlined in the Methods section. Additionally, the high quality of plasma was confirmed by undetectable levels of erythrocytes and platelets on a routine haematology analyser before freezing. Furthermore, we spectophotometrically determined free haemoglobin concentrations in the thawed plasma samples, which were found to be well below the levels indicative of haemolysis, and assessed plasma PF4 levels by ELISA at 1468 (781–2370) ng/mL (median [25%–75%]), as an indicator of platelet activation level (Tables S8 and S9, Figure S2; MIBlood-EVs).

### 3.2 | Cell-Specific Circulating EV Subsets Show a Wide Range of Concentrations Independent of Cell-of-Origin Levels in Blood

To identify the cellular origins of circulating EVs in healthy adults, we next performed phenotyping of EV-surface proteins

**TABLE 1** | Study subject's characteristics.

| | Unit/Category | Median (25%–75%) | *N* (%) |
|---|---|---|---|
| Sex | Male | | 104 (50.0) |
| | Female | | 104 (50.0) |
| Age | All subjects/years | 44.5 (29.3–54.8) | |
| | 18–29 years | | 52 (25.0) |
| | 30–44 years | | 52 (25.0) |
| | 45–54 years | | 52 (25.0) |
| | 55–65 years | | 52 (25.0) |
| Weight[a] | kg | 78 (66–87) | |
| Height[a] | m | 1.74 (1.68–1.80) | |
| Body mass index | $kg/cm^2$ | 25.6 (22.8–28.1) | |
| Body temperature | °C | 36 (35.7–36.2) | |
| Systolic blood pressure | mmHg | 136 (121–145) | |
| Diastolic blood pressure | mmHg | 78 (71–86) | |
| Heart rate | beats/min | 78 (69–86) | |
| Serum ApoA1 | mg/mL | 1.62 (1.49–1.79) | |
| Serum ApoB | mg/mL | 0.90 (0.74–1.08) | |
| Serum Insulin[b] | μU/mL | 13.2 (7.9–23.9) | |
| Serum hsCRP | μg/mL | 0.74 (0.38–1.56) | |
| Smoking[a] | No | | 148 (71.2) |
| | Yes | | 60 (28.8) |
| Exercise intensity[a] | Moderate | | 173 (83.2) |
| | Intensive | | 35 (16.8) |
| Exercise frequency[a] | <2–3×/week | | 157 (75.5) |
| | >2–3×/week | | 51 (24.5) |
| Time passed since the last exercise[a] | < 12 h | | 13 (6.3) |
| | 12–24 h | | 23 (11.1) |
| | 24–48 h | | 14 (6.7) |
| | > 48 h | | 158 (76.0) |

Abbreviations: ApoA1—apolipoprotein A1; ApoB—apolipoprotein B; hsCRP—highly sensitive measurement of C-reactive protein.

[a]self-reported data.

[b]in 34 samples values were below the limit of detection (3.06 μU/mL), only subjects with values larger than 3.06 μU/mL were included in the calculation of the median.

by imaging flow cytometry directly in the defrosted plasma. Specifically, we determined concentrations of circulating EV subsets carrying one of the 25 studied markers of different blood or endothelial cells, delineated in Figure 2a and Table S1. Some of the analysed markers also indicate precursor or stem cells. However, their percentage among circulating total nucleated cells in healthy adults at a steady state is less than 0.1% (Körbling and Anderlini 2001), so we inferred the precursor or stem cells are unlikely to be an important source of circulating EVs in our study. All investigated EV subsets, besides CD44+ EVs, were detected in the plasma of more than 95% of subjects, but showed a wide range of concentrations, from 4.2 (0.8–12) × $10^7$/mL to 1.9 (1.2–4.4) × $10^5$/mL (median [25%–75%]; Figure 2b; Table 2). Circulating EV subsets with the highest median concentrations were positive for GPIIb/IIIa*, HLA-ABC, CD9, phosphatidylserine (PS), or CD227, while those with the lowest were positive for CD62P, CD90, CD13, CD14, CD44, or CD24.

To estimate the relative abundance of circulating EV subsets with respect to their cell origin, we used established markers for the immunophenotyping by flow cytometry (Kalina et al. 2019; Grant et al. 2021; de Oliveira, Welsh, and Pinckney 2023; Berckmans et al. 2019; Spurgeon and Frelinger 2022). We designated CD235a+ subsets as erythrocyte EVs, CD41+ and GPIIb/IIIa*+ subsets as platelet EVs, and CD61 EVs as originating from mostly platelets, but also from leukocytes or endothelial cells. CD62P+ EVs, on the other hand, are associated with activated platelets and activated endothelial cells, and serve as an established marker of platelet activation. CD31+ EVs are primarily associated with endothelial cells but can also be detected on platelets and leukocytes.

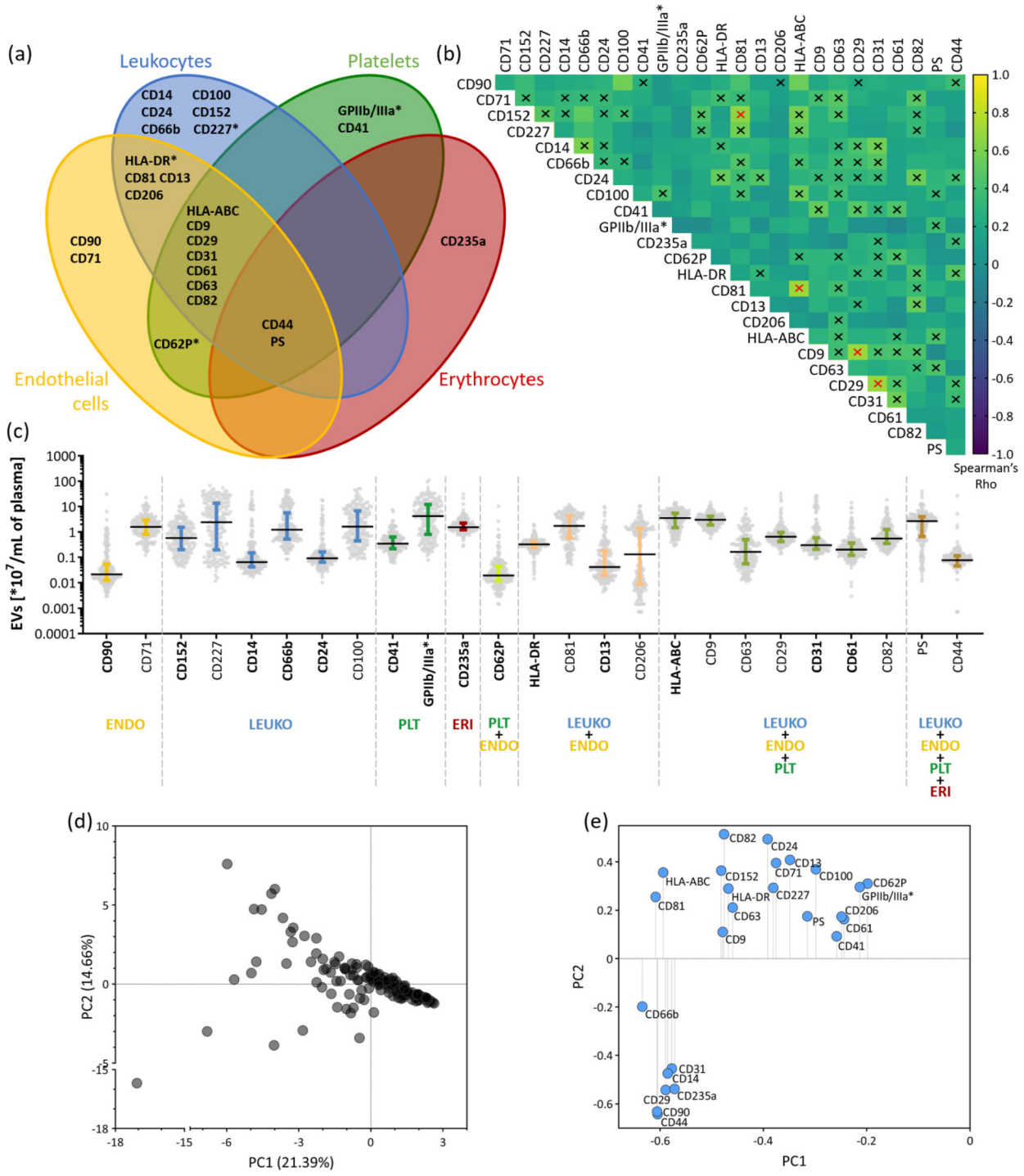


**FIGURE 2** | Quantification of circulating EV subsets with respect to their cell of origin in the plasma of healthy humans by imaging flow cytometry. (a) Representation of surface protein markers, included in imaging flow cytometry analysis, with respect to their presence on specific blood cell types. * indicates cell activation markers. (b) The measured concentrations of analysed circulating EV subsets, reported as median with interquartile range. Each dot represents one sample. Characteristic markers for the individual cell type are indicated in bold. ENDO—endothelial cells; LEUKO—leukocytes; PLT—platelets; ERI—erythrocytes. (c) Spearman's correlations across all circulating EV subsets. Black cross—$\rho$: 0.3 – 0.59, Red cross—$\rho \geq 0.6$. All depicted correlations are also statistically significant. (d) Principal component 1 vs. 2 (PC1 vs. PC2) graph of the principal component analysis (PCA). Each dot represents one study subject. PC1 captures the most significant variation in the data, thus distances along the PC1 axis represent a larger variation than the same distances along the PC2 axis. (e) Loadings of original variables (circulating EV subset concentrations) of PCA. Circulating EV subsets with larger absolute values give the largest contribution to PC1 and PC2.

**TABLE 2** | Concentrations of EV subsets, carrying cell-specific surface markers, in the plasma of healthy humans as measured by imaging flow cytometry.

| Marker | × $10^7$/mL of plasma Median (25%–75%) Total | × $10^7$/mL of plasma Median (25%–75%) Male | × $10^7$/mL of plasma Median (25%–75%) Female | % CV Total (male/female) | *N* Total (male/female) |
|---|---|---|---|---|---|
| **CD90** | 0.021 (0.012–0.054) | 0.019 (0.012–0.042) | 0.026 (0.014–0.055) | 719 (215/663) | 200 (98/102) |
| **CD71** | 1.580 (0.809–2.905) | 1.525 (0.785–2.748) | 1.6 (0.826–3.095) | 116 (102/123) | 200 (98/102) |
| **CD152** | 0.577 (0.204–1.505) | 0.386 (0.163–1.405) | 0.786 (0.277–1.800) | 162 (131/163) | 200 (98/102) |
| **CD227** | 2.410 (0.197–13.400) | 1.54 (0.152–13.050) | 3.21 (0.289–12.650) | 143 (146/141) | 200 (98/102) |
| **CD14** | 0.064 (0.042–0.150) | 0.062 (0.039–0.097) | 0.076 (0.048–0.236) | 353 (334/349) | 200 (98/102) |
| **CD66b** | 1.225 (0.528–5.540) | 1.01 (0.438–4.068) | 1.345 (0.581–6.135) | 169 (175/163) | 200 (98/102) |
| **CD24** | 0.091 (0.065–0.163) | 0.081 (0.057–0.132) | 0.105 (0.069–0.177) | 358 (413/319) | 200 (98/102) |
| **CD100** | 1.625 (0.451–6.170) | 1.645 (0.328–5.773) | 1.625 (0.517–7.648) | 164 (161/161) | 200 (98/102) |
| **CD41** | 0.344 (0.218–0.626) | 0.338 (0.201–0.610) | 0.359 (0.231–0.650) | 138 (137/138) | 200 (98/102) |
| **GPIIb/IIIa*** | 4.185 (0.817–11.950) | 1.75 (0.575–7.575) | 6.29 (1.805–15.775) | 153 (153/139) | 200 (98/102) |
| **CD235a** | 1.540 (1.218–2.225) | 1.64 (1.223–2.550) | 1.5 (1.213–2.028) | 127 (102/150) | 200 (98/102) |
| **CD62P** | 0.019 (0.012–0.044) | 0.018 (0.012–0.043) | 0.022 (0.011–0.044) | 637 (201/560) | 200 (98/102) |
| **HLA-DR** | 0.322 (0.241–0.420) | 0.331 (0.234–0.382) | 0.313 (0.25–0.475) | 70 (64/74) | 200 (98/102) |
| **CD81** | 1.730 (0.617–4.220) | 1.36 (0.507–3.908) | 2.615 (0.902–4.770) | 93 (104/83) | 200 (98/102) |
| **CD13** | 0.042 (0.020–0.175) | 0.056 (0.024–0.198) | 0.034 (0.018–0.126) | 337 (359/295) | 200 (98/102) |
| **CD206** | 0.215 (0.009–1.438) | 0.052 (0.007–1.348) | 0.719 (0.013–1.460) | 161 (183/122) | 197 (96/101) |
| **HLA-ABC** | 3.520 (1.468–5.445) | 2.795 (1.193–5.198) | 4.06 (1.728–6.560) | 74 (77/69) | 200 (98/102) |
| **CD9** | 2.995 (1.870–4.125) | 2.745 (1.883–3.990) | 3.125 (1.765–4.290) | 63 (66/60) | 200 (98/102) |
| **CD63** | 0.163 (0.057–0.504) | 0.103 (0.045–0.422) | 0.212 (0.078–0.552) | 182 (182/179) | 200 (98/102) |
| **CD29** | 0.646 (0.417–0.950) | 0.641 (0.389–0.896) | 0.654 (0.487–1.118) | 254 (196/262) | 200 (98/102) |
| **CD31** | 0.304 (0.211–0.581) | 0.291 (0.194–0.505) | 0.326 (0.229–0.689) | 260 (272/248) | 200 (98/102) |
| **CD61** | 0.203 (0.121–0.367) | 0.187 (0.123–0.322) | 0.212 (0.120–0.408) | 261 (241/281) | 199 (98/101) |
| **CD82** | 0.5.46 (0.3.52–1.2.35) | 0.5.94 (0.3.68–1.4.95) | 0.5.3 (0.3.27–0.9.33) | 159 (160/157) | 200 (98/102) |
| **PS** | 2.675 (0.679–3.950) | 2.085 (0.461–3.613) | 2.995 (1.155–4.170) | 136 (173/99) | 200 (98/102) |
| **CD44** | 0.090 (0.064–0.123) | 0.096 (0.070–0.123) | 0.08 (0.062–0.128) | 680 (132/613) | 169 (77/92) |

*Note:* Markers shaded in grey are the most characteristic markers of the individual cell type.

Additionally, CD90+ EVs were identified as originating from activated endothelial cells in our study (Wandel et al. 2012), as we do not expect precursor or stem cells to be an important source of circulating EVs (Körbling and Anderlini 2001). Among leukocytes, CD66+ EVs originate from activated granulocytes, CD152+ EVs from T lymphocytes, and CD24+ EVs from B lymphocytes or granulocytes. Antigen-presenting cells (APCs) were associated with HLA-DR+ EVs, while CD14+ subsets were identified as monocyte EVs.

When considering the median concentrations of cell-specific EV subsets (Figure 2b, Table 2), activated platelet EVs emerged as the most abundant among circulating EVs, followed by erythrocyte EVs, granulocyte EVs, T lymphocyte EVs, EVs from APCs (including monocyte EVs), and endothelial EVs in the lowest concentration. We investigated the relationship between circulating EV subset concentrations and their corresponding cells-of-origin, as determined by complete blood count (Table S7). No statistically significant correlation was found. Notably, both the highest (GPIIb/IIIa*+) and lowest (CD62P+) median concentrations of circulating EV subsets originated mostly from activated platelets. To further explore possible patterns among EV subsets, we assessed correlations among all 25 EV subset concentrations (Figure 2c). We identified only four moderate associations ($\rho > 0.6$, marked with a red cross in Figure 2c), suggesting steady-state EV subset concentrations are regulated by complex mechanisms, which differ even for EV subsets from the same cell type.

Furthermore, we performed the PCA to independently identify similarities among study subjects based on their circulating EV subsets concentrations. Principal components PC1 and PC2 revealed a compact cluster of study subjects, suggesting high multidimensional similarity in their circulating EV subset concentrations. The remaining study subjects appeared scattered, lacking distinct patterns or clusters (Figure 2d). Loadings in PCA represent the contribution of each variable to each principal component, revealing the most influential variables in explaining data variance. In our analysis, granulocyte-derived CD66b+ EVs, CD81+ EVs, activated endothelial CD90+ EVs, and CD44+ EVs contributed most to the variation observed in the PC1 component (Figure 2e). EV subsets derived mostly from platelets (CD41+, CD61+, GPIIb/IIIa*+, and CD62P+ EVs) formed a distinct cluster in the loadings graph of PCA, yet their contribution to PC1 variation was minimal. Additionally, among three of the most commonly studied EV-related tetraspanins, CD9+ and CD63+ EVs showed similar loadings on PC1, distinct from the CD81+ EVs.

Altogether, we characterized circulating EVs under physiological conditions with respect to their cellular source in the plasma of healthy humans. EV subset concentrations did not reflect concentrations of cells-of-origin in blood, suggesting complex regulation mechanisms of their steady-state concentrations that differ even for EV subsets from the same cell type.

### 3.3 | Total Particle Quantification of EV Samples Enriched From Plasma of Healthy Humans

We detected high median concentrations of circulating EV subsets, positive for tetraspanins CD9 and CD81, while CD63+ EV concentration was much lower. To investigate the cellular origin of those tetraspanin+ circulating EVs, we first enriched EVs from the plasma of all study subjects using established sucrose cushion ultracentrifugation (Figure 1; Holcar et al. 2020). As evaluated by NTA, the median (25%–75%) mean concentration of particles in enriched EV samples across study subjects was $5.65 \times 10^9$ ($5.07–6.19 \times 10^9$) particles/mL of plasma, with median (25%–75%) modal diameter of 151.7 (144.8–158.9) nm (Figure S3a,b). At the same time, ELISA showed a substantial decrease of ApoA1 and ApoB levels after enrichment of EVs from the subject's plasma (Figure S2; 0.0057% and 0.0017% [with 92 samples below the limit of detection] of ApoA1 and ApoB, respectively). A statistically significant difference in the NTA-detected particle concentrations was observed between sexes ($5.74 \times 10^9$ and $5.44 \times 10^9$ particles/mL for males and females, respectively; $p = 0.01715$, Figure S3c). However, this difference was within the calculated analytical CV for NTA concentration measurements of 7.89%, equivalent to $0.45 \times 10^9$ particles/mL (Figure S3d). Therefore, it might be attributed to the imprecision inherent in NTA concentration measurements rather than holding biological importance.

### 3.4 | Tetraspanin+ Circulating EVs Largely Originate From Platelets and Lymphocytes in the Plasma of Healthy Humans

We next performed phenotyping of EVs based on their expression of 37 surface proteins with semi-quantitative multiplex bead-based flow cytometry on enriched circulating EVs across study subjects (Figure 1). Specifically, we determined normalized median fluorescence intensity (MFI) as a measure of the expression level of cell-type specific protein markers (delineated in Figure 3a, Table S10), present on the surface of circulating CD9 and/or CD81 and/or CD63 positive (tetraspanin+) EVs (Figure 3). Twenty-three markers were detected in the plasma of more than 91% of subjects and included in further analysis, showing up to a 17-fold difference in the level of expression on the tetraspanin+ circulating EVs (from 19.63 [11.59–29.21] to 1.13 [0.85–1.66] normalized median MFI [25%–75%]; Figure 3b, Table 3). Thirteen surface protein markers were excluded from the analysis due to low detection across study subjects (measured MFIs were in the range of or under the limit of detection), while ROR1 surface protein was excluded as it is a cancer marker.

Tetraspanin+ circulating EVs showed the highest expression levels for mostly platelet markers CD41b, CD62P, and CD42a, alongside the more general marker CD29 and leukocyte protein HLA-DRDPDQ. Conversely, expression was the lowest for lymphocyte markers CD2 and CD69 and the endothelial marker CD146. Other evaluated markers with intermediate expression were leukocyte markers CD8 (lymphocyte T), CD45, CD24 (lymphocyte B or granulocytes), CD3 (lymphocyte T), CD14 (monocytes), CD105 (macrophages and endothelium), and CD4 (mostly lymphocyte T), ranked from highest to lowest. Additionally, more general markers of blood cells, such as HLA-ABC (present on all nucleated blood cells), CD44, CD1c, CD31 and CD40, demonstrated intermediate expression on tetraspanin+ circulating EVs (Figure 3b, Table 3). Erythrocyte-specific markers are not included in this multiplex bead-based flow cytometry analysis. Additional analyses of correlations between different

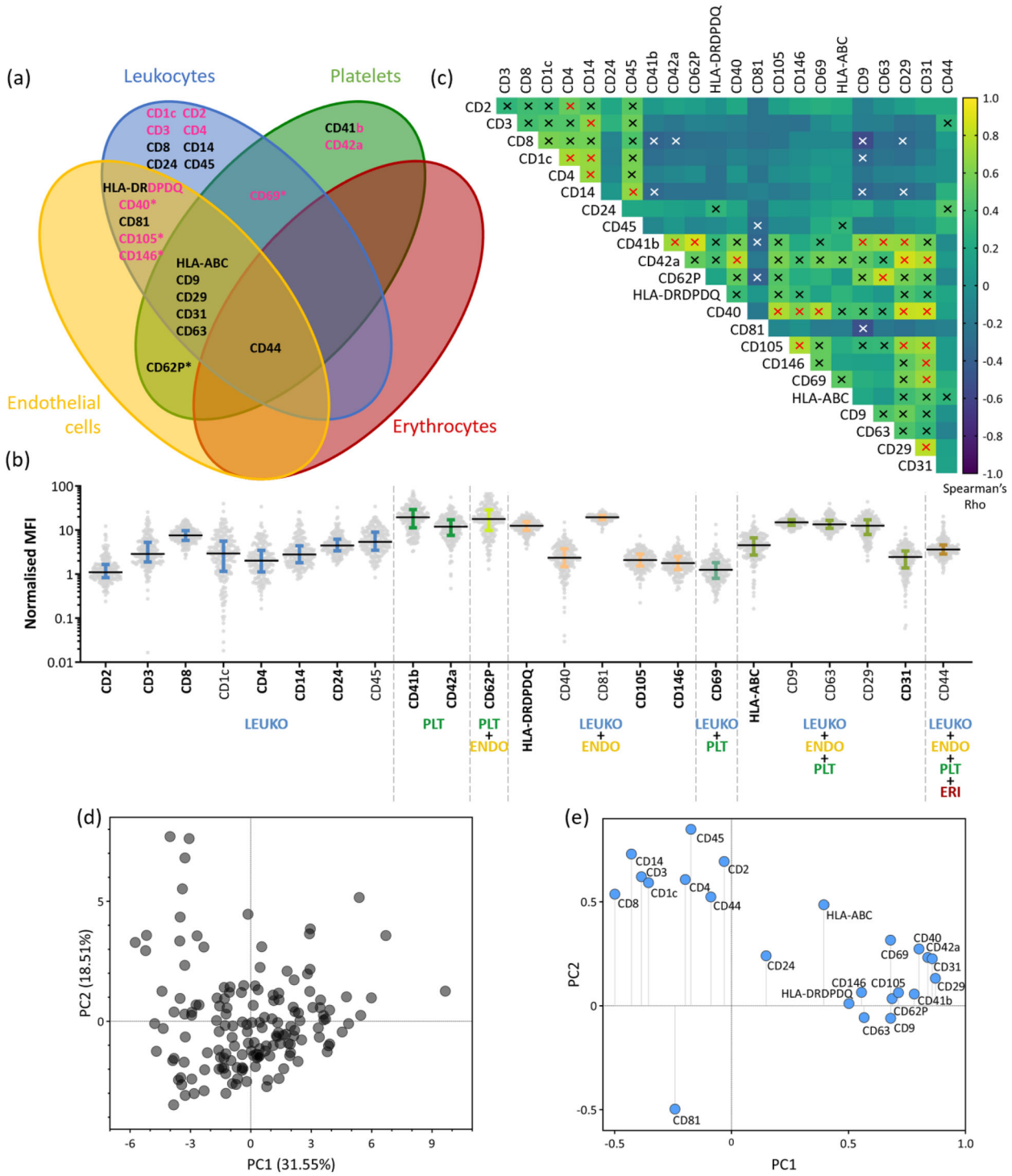


**FIGURE 3** | Quantification of expression levels of cell-type specific markers on circulating tetraspanin+ EVs enriched from plasma of healthy humans, as determined by multiplex bead-based flow cytometric analysis. (a) Representation of surface protein markers included in multiplex bead-based flow cytometric analyses with respect to their presence on specific blood cell types. * indicates cell activation markers. Black text indicates markers were also included in the imaging flow cytometry analysis, while those in pink were only analysed by multiplex bead-based FC. (b) Normalized median fluorescence intensity (MFI) of tetraspanin+ circulating EVs expressing one of the studied markers, reported as median with interquartile range. Each dot represents one sample. Characteristic markers for the individual cell type are indicated in bold. ENDO—endothelial cells; LEUKO—leukocytes; PLT—platelets; ERI—erythrocytes. (c) Spearman's correlation across all tetraspanin+ circulating EVs expressing specific markers. Black cross—$\rho$: 0.3–0.59, Red cross—$\rho \geq 0.6$, White cross—$\rho \leq -0.3$. All correlations were statistically significant. (d) Principal component 1 vs. 2 (PC1 vs. PC2) graph of the principal component analysis (PCA). Each dot represents one study subject. PC1 captures the most significant variation in the data, thus distances along the PC1 axis represent a larger variation than the same distances along the PC2 axis. (e) Loadings of original variables (circulating EV subset concentrations) of PCA. Tetraspanin+ circulating EVs with larger absolute values give the largest contribution to PC1 and PC2.

**TABLE 3** | Expression levels of cell-type specific markers on tetraspanin+ circulating EVs in the plasma of healthy humans as measured by multiplex bead-based flow cytometry.

| Marker | Normalised MFI Median (25%–75%) total | Normalised MFI Median (25%–75%) Male | Normalised MFI Median (25%–75%) Female | % CV Total (male/female) | *N* Total (male/female) |
|---|---|---|---|---|---|
| **CD2** | 1.13 (0.85–1.66) | 1.09 (0.78–1.61) | 1.21 (0.9–1.94) | 91 (63/100) | 191 (95/96) |
| **CD3** | 2.91 (1.93–5.33) | 3.08 (1.95–5.37) | 2.85 (1.85–5.33) | 87 (90/83) | 199 (99/100) |
| **CD8** | 7.61 (5.93–9.75) | 7.81 (6.25–9.47) | 7.13 (5.79–9.8) | 38 (37/38) | 205 (103/102) |
| **CD1c** | 3.20 (1.45–6.15) | 3.2 (1.68–5.95) | 2.98 (1.18–6.24) | 107 (90/119) | 189 (92/97) |
| **CD4** | 2.05 (1.18–3.51) | 2.06 (1.21–3.13) | 2.03 (1.15–3.78) | 111 (79/127) | 196 (97/99) |
| **CD14** | 2.85 (1.85–4.41) | 2.97 (2.04–4.56) | 2.66 (1.65–4.35) | 93 (90/97) | 202 (100/102) |
| **CD24** | 4.46 (3.39–6.10) | 4.25 (3.38–5.75) | 4.69 (3.44–6.84) | 64 (56/69) | 205 (102/103) |
| **CD45** | 5.48 (3.52–90) | 5.3 (3.49–9.62) | 5.73 (3.61–8.33) | 67 (63/71) | 205 (102/103) |
| **CD41b** | 19.63 (11.59–29.21) | 20.06 (11.16–28.58) | 19.39 (11.77–29.52) | 61 (62/60) | 205 (103/102) |
| **CD42a** | 12.00 (7.86–17.22) | 11.95 (7.54–16.43) | 12.85 (8.24–17.84) | 57 (62/53) | 205 (103/102) |
| **CD62P** | 17.9 (10.08–28.93) | 17.55 (8.22–27.2) | 18.35 (12.75–30.52) | 72 (79/66) | 205 (103/102) |
| **HLA-DRDPDQ** | 12.6 (10–15.48) | 12.6 (10.63–15.65) | 12.55 (9.86–15.21) | 32 (32/32) | 205 (103/102) |
| **CD40** | 2.42 (1.59–3.85) | 2.45 (1.55–3.69) | 2.39 (1.62–4.06) | 67 (74/59) | 196 (100/96) |
| **CD81** | 19.5 (17.32–21.54) | 19.5 (17.52–21.18) | 19.5 (17.3–21.79) | 16 (17/16) | 206 (103/103) |
| **CD105** | 2.13 (1.54–2.87) | 2.28 (1.62–3.07) | 2.07 (1.44–2.63) | 43 (41/45) | 197 (100/97) |
| **CD146** | 1.79 (1.29–2.48) | 1.75 (1.26–2.36) | 1.9 (1.3–2.53) | 51 (52/50) | 196 (99/97) |
| **CD69** | 1.26 (0.8–1.81) | 1.26 (0.79–1.81) | 1.26 (0.8–1.79) | 85 (97/69) | 195 (99/96) |
| **HLA-ABC** | 4.63 (3.09–6.87) | 4.65 (3.32–6.78) | 4.62 (2.75–6.91) | 57 (63/49) | 194 (99/95) |
| **CD9** | 15.08 (12.94–17.34) | 15.05 (12.79–17.11) | 15.1 (13.2–17.73) | 24 (26/22) | 206 (103/103) |
| **CD63** | 13.59 (11.05–16.55) | 12.4 (10.57–15.69) | 14.36 (11.8–17.42) | 36 (39/33) | 206 (103/103) |
| **CD29** | 12.63 (7.98–17.2) | 12.66 (7.74–17.05) | 12.63 (8.95–17.28) | 49 (52/47) | 206 (103/103) |
| **CD31** | 2.51 (1.51–3.38) | 2.41 (1.37–3.33) | 2.59 (1.73–3.39) | 60 (67/53) | 196 (99/97) |
| **CD44** | 3.65 (2.88–4.61) | 3.68 (3.03–4.82) | 3.48 (2.82–4.57) | 59 (64/52) | 205 (102/103) |

[a]Markers, shaded in grey are the most characteristic markers of representative cell type.

markers of mostly activated platelets (CD62P+ EVs, PF4 concentration) and concentration of platelets in whole blood or plasma excluded non-physiological platelet activation after the blood draw (Figure S2). Importantly, examination of normalized expression levels (measured by multiplex bead-based flow cytometry) or normalized concentrations (measured by imaging flow cytometry) of markers CD14, CD24, CD41, CD62P, HLA-DR, HLA-ABC, CD29, CD31, and CD44 on circulating EVs revealed distinct profiles for tetraspanin+ circulating EVs compared to the overall circulating EV population (Figure S4). Thus, tetraspanin+ circulating EVs are not representative of the entire circulating EV population in healthy human plasma.

To determine if markers specific to a particular cell type exhibited similar expression patterns on tetraspanin+ circulating EVs, we evaluated correlations among the 23 studied surface proteins (Figure 3c) and found 26 pairs with moderate correlations ($\rho >$ 0.6, red cross). Among those, CD41b expression correlated with CD42a, CD62P, CD9 and CD63 ($\rho > 0.6$, red cross), indicating a conserved pattern of marker expression on CD9+ and/or CD63+ EVs released from platelets across study subjects. Similarly, the expression of CD105 correlated with CD146, CD31, and CD29, indicating a conserved pattern of marker expression on tetraspanin+ circulating EVs released from endothelium. For leukocyte markers, we mostly observed individual correlations (e.g., CD2 with CD4; CD14 with CD3, CD4, and CD45), which might reflect the diversity of leukocyte cell types.

We conducted PCA to assess similarities among study subjects based on the expression levels of all studied surface markers on tetraspanin+ circulating EVs (Figure 3d). Subjects were less tightly clustered when compared to the PCA analysis of circulating EV subset concentrations (Figure 2d). Expression levels of markers CD29 and CD31 (both cell-type nonspecific), followed by CD42a and CD40 (typical for B lymphocytes, macrophages, and dendritic cells) on tetraspanin+ circulating EVs, influenced most of the variation observed in the PC1 component (Figure 3e). CD9+ and CD63+ EVs showed similar loadings on PC1, while CD81+ EVs diverged significantly, indicating distinct cell origins for the latter.

In summary, tetraspanin+ circulating EVs in healthy humans largely originate from platelets and to a lesser extent from lymphocytes, while some also originate from other leukocyte types or endothelium. Interestingly, studied platelet or endothelial markers show a conserved pattern of expression on tetraspanin+ circulating EVs across study subjects.

### 3.5 | Circulating EVs Show High Inter-Individual Biological Variation in Healthy Humans

While high inter-individual biological variation is commonly observed in established plasma analytes, it has yet to be studied for circulating EVs. To assess inter-individual biological variation in the concentration of circulating EV subsets, positive for one of the 25 studied markers of different blood cells or endothelial cells, we calculated the CV across all study subjects (Figure 4a, Table 2). Inter-individual variation was high for all circulating EV subset concentrations (median CV across all EV subsets was 162%) but varied a lot between different EV subsets. Circulating CD90+, CD44+, and CD62P+ EV concentrations had a CV of 719%, 680%, and 637%, respectively, while CD9+, HLA-DR+, HLA-ABC+, and CD81 EV concentrations were more consistent across study subjects (63%, 70%, 74%, and 93%, respectively). Interestingly, high inter-individual variation observed for circulating CD90+, CD44+, and CD62P+ EVs was mostly at the expense of high CVs observed in females (663%, 613%, and 560%, respectively, Figure S5a). CV was inconsistent across different EV subsets originating from the same cell type, and independent of activation state across various cell types. For example, CD41+, GPIIb/IIIa*+, and CD62P+ EV subsets originating mostly from platelets had CVs of 138%, 153%, and 637%, respectively. Similarly, CD90+, CD66b+, GPIIb/IIIa*+, and CD62P+ EV subsets, originating from activated endothelial cells, granulocytes and platelets, respectively, had CVs in the range of 719% to 153%.

The expression level (normalized median MFI) of 23 cell-type specific protein markers on the surface of tetraspanin+ circulating EVs, was much more consistent across study subjects (median CV across all EV subsets was 60%; Figure 4b, Table 3) compared to the concentration of circulating EV subsets. Still, higher inter-individual variation was observed for CD4, CD1c, CD14, and CD2 expression on tetraspanin+ circulating EVs (CVs of 111%, 107%, 93%, and 91%, respectively), while the lowest was observed for HLA-DRDPDQ, CD8, and CD105 (CVs of 32%, 38%, and 43%, respectively). Again, high inter-individual variation was driven by higher CVs in females (127% for CD4, 119% for CD1c, and 100% for CD2; Figure 4b, Table 3, and Figure S5b).

Taken together, circulating EV subset concentrations show high inter-individual biological variation in healthy humans, with differing levels of variation for EV subsets originating from the same cell type or with respect to its activation state. In comparison, the tetraspanin+ circulating EVs show lower variation in expression levels of cell-type specific protein markers.

### 3.6 | Sex, Menopausal Status and Smoking Contribute to Inter-Individual Biological Variation of Specific Circulating EV Subsets, Originating From Platelets, Leukocytes, or Erythrocytes

Our study of inter-individual variation of circulating EV subset concentrations indicated sex could be one of the underlying factors of this variation. To comprehensively investigate the sources of observed biological variation, we collected data on the following demographic (age, sex), clinical (height, weight, body mass index, blood pressure, blood pulse, menopause status, complete blood count and lipoprotein concentrations), and lifestyle (exercise regimen, time since last exercise, smoking status) factors across the study subjects (Table 1) and analysed their association with measured circulating EV subset concentrations.

The heatmap visually represents all measured circulating EV subset concentrations for every study subject. We arranged them by increasing age, sex, menopausal status, and smoking (Figure 5a). There is a visible pattern of higher EV concentrations for most EV subsets in pre- and peri-menopausal females, compared to post-menopausal females or males. Importantly, the PCA showed none of the analysed subject's factors significantly influenced the measured concentrations of the 25 circulating EV subsets on a global level. However, we identified sex, menopausal status, and

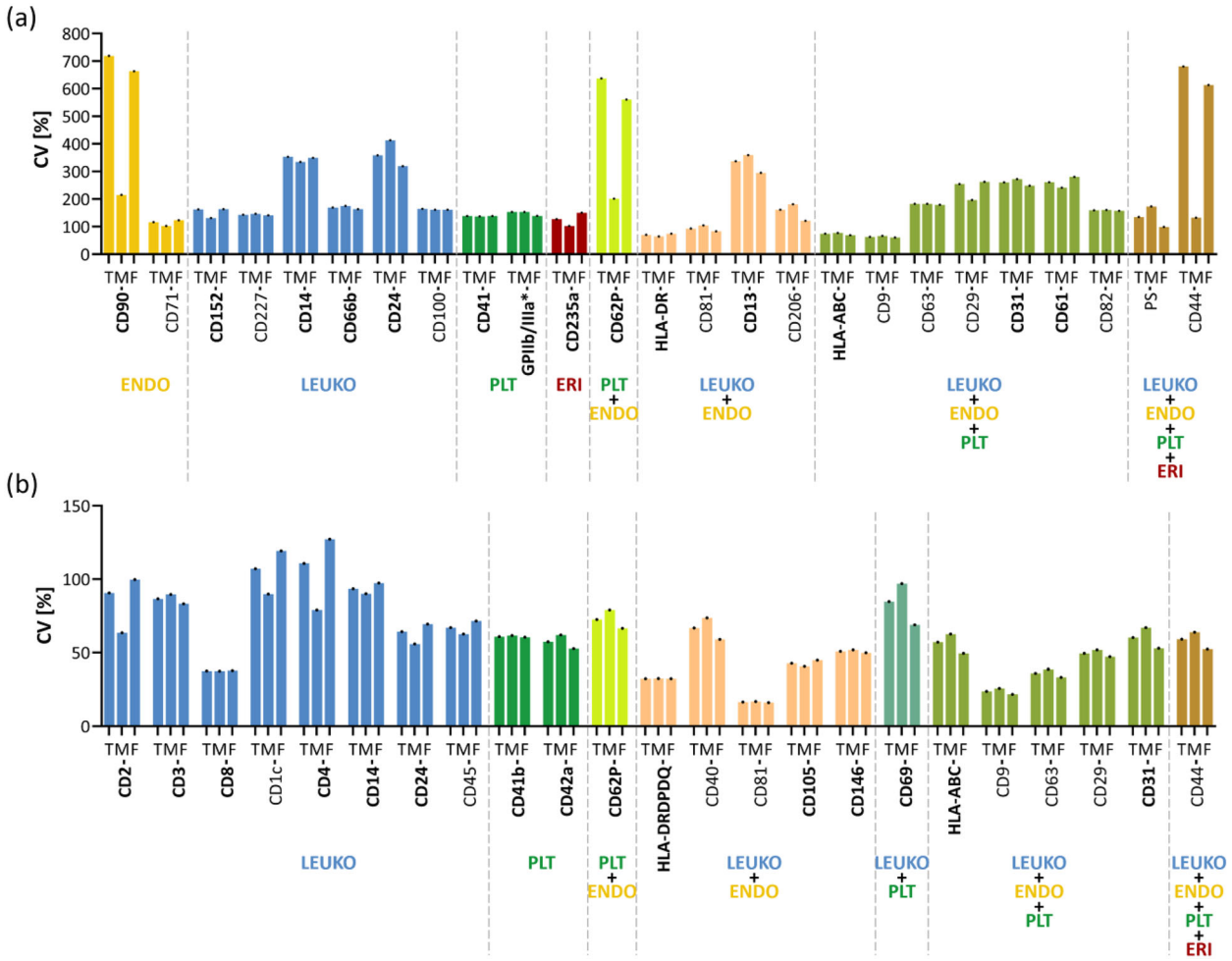


**FIGURE 4** | Analysis of inter-individual biological variation of circulating EV subset concentrations and marker expression levels on tetraspanin+ circulating EVs. Coefficient of variations of (a) circulating EV subset concentrations and (b) normalized MFI for markers on tetraspanin+ circulating EVs, across study subjects. CV—coefficient of variation; T—total; M—male; F—Female; ENDO—endothelial cells; LEUKO—Leukocytes; PLT—platelets; ERI—erythrocytes.

smoking as factors associated with specific circulating EV subset concentrations, as detailed below (Figure 5b–l).

Although sex did not result in distinct groupings in PCA of EV subset concentrations (Figure 5b), platelet GPIIb/IIIa*+ EVs exhibited significantly higher concentrations in females compared to males ($p$ = 0.00010, Figure 5c). This could not be attributed to differences in platelet concentrations in whole blood or free PF4 levels in plasma, as no significant differences were observed between females and males (Figure 5d,e).

When data represented on the PCA graph was color-coded by menopausal status, no distinct patterns were observed (Figure 5f). However, CD66b+, CD100+, and CD152+ EVs, originating from granulocytes, leukocytes, and T lymphocytes, respectively, exhibited significantly higher concentrations in pre-menopausal females compared to post-menopausal ones ($p$ = 0.00109, $p$ = 0.00001, and $p$ = 0.00068, respectively; Figure 5g). Notably, blood leukocyte, lymphocyte, or neutrophil concentrations were not dependent on female menopausal status (Figure 5h).

Finally, although smoking did not have global influence on concentration of circulating EV subsets according to PCA (Figure 5i), CD235a+ EVs originating from erythrocytes, showed significantly lower concentrations in smokers compared to non-smokers ($p$ = 0.00009, Figure 5j). This could not be explained by the influence of smoking on blood erythrocyte levels or haemolysis, since no significant differences were observed across study subjects (Figure 5k,l).

To conclude, no global influence on studied circulating EV subsets was observed for any of the subject's factors. However, sex, menopausal status, and smoking were shown to contribute to inter-individual biological variation of specific circulating EV subsets, originating from platelets, leukocytes, or erythrocytes, respectively.

### 3.7 | Smoking and Age Contribute to Inter-Individual Biological Variation in Levels of Specific Protein Markers of Platelets, Leukocytes or Endothelial Cells Expressed on Tetraspanin+ Circulating EVs

The tetraspanin+ circulating EVs exhibited lower biological variation in the expression levels of cell-type specific protein

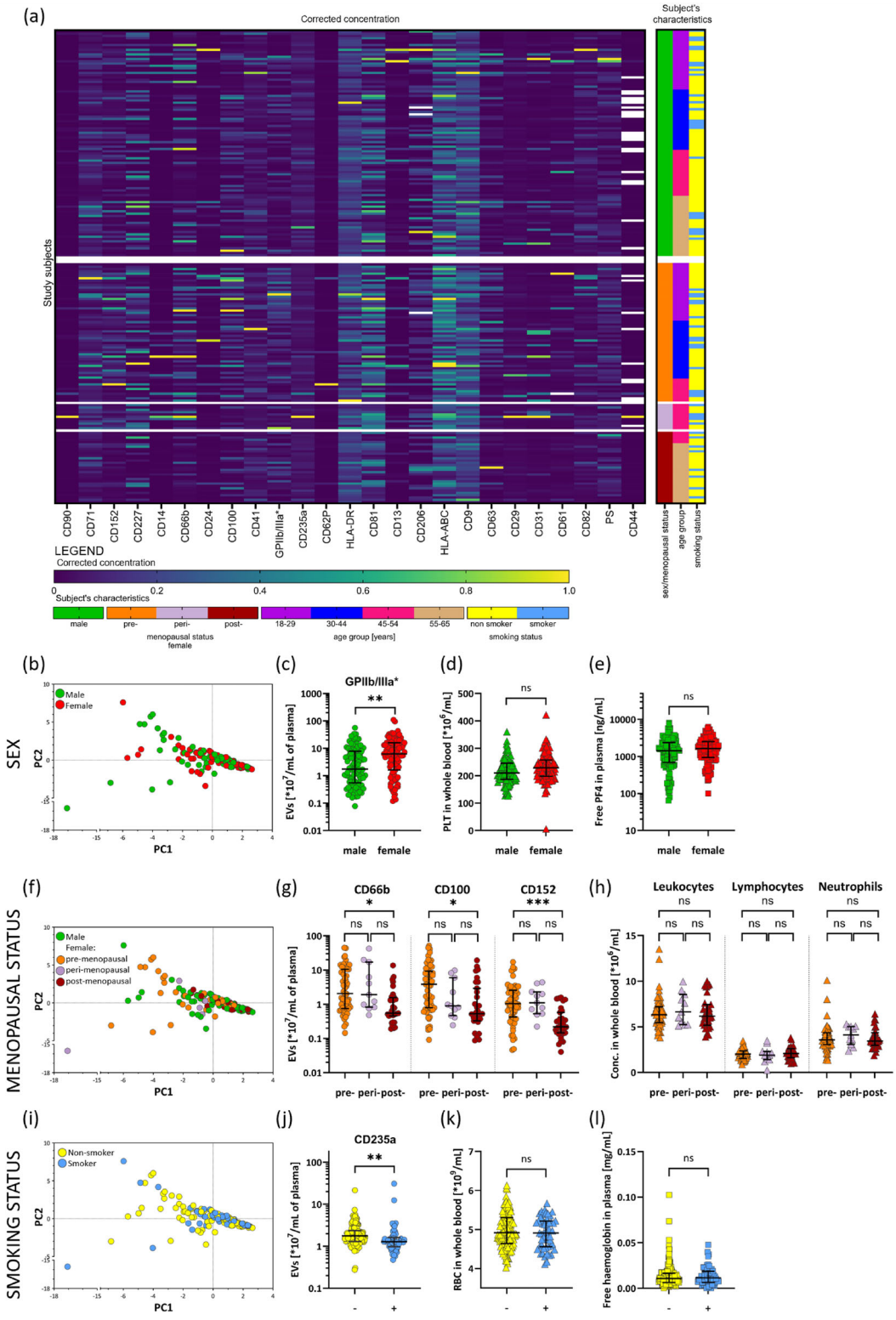


**FIGURE 5** | Sources of inter-individual biological variation observed in circulating EV subsets. (a) Results of imaging flow cytometry analysis of circulating EV subsets, normalized to the largest measured value of each circulating EV subset. Each line represents one study subject. Subjects are arranged by their increasing age, sex, menopausal status and smoking status. (b) PCA plot, coloured according to the sex of study subjects. Influence of sex on (c) concentration of GPIIb/IIIa*+ circulating EVs in plasma, (d) concentration of platelets in whole blood and (e) concentration of free PF4 in plasma. (f) PCA plot, coloured according to the menopausal status of study subjects. Influence of menopause status on concentrations of (g) CD66b+, CD100+ and CD152+ circulating EVs in plasma, and (h) concentration of leukocytes, lymphocytes and neutrophils in whole blood. (i) PCA plot, coloured according to the smoking status of study subjects. Influence of smoking on (j) concentration of CD235a+ circulating EVs in plasma, (k) concentration of erythrocytes in whole blood, and (l) concentration of free haemoglobin in plasma. Each dot represents one study subject. Black lines represent the median with the interquartile range. *—$p < 0.002$; **—$p < 0.0004$; ***—$p < 0.00004$; ns—nonsignificant; PLT—platelets, PF4 – platelet factor 4; RBC—erythrocytes; WBC—leukocytes.

markers, in comparison to the observed variation in circulating EV subset concentrations. However, their CVs still ranged from 32% to 111%, prompting us to investigate the factors contributing to this variation. The heatmap visually represents all measured expression levels of markers on tetraspanin+ circulating EVs for every study subject, which are arranged by increasing age, sex, menopausal status, and smoking (Figure 6a). We next examined the contribution of individual subject factors (Table 1) to variation in the expression levels of cell-type specific protein markers on tetraspanin+ circulating EVs. Again, none of the analysed subjects' factors significantly influenced the observed variation on a global level. However, association analysis revealed that smoking and age were correlated with the expression levels of specific protein markers present on the surface of tetraspanin+ circulating EVs as detailed below (Figure 6b–j).

While smoking did not show distinct clusters in PCA (Figure 6b), it did affect the expression levels of eight protein markers on tetraspanin+ circulating EVs. Median normalized MFI levels of five of these markers (CD29, a nonspecific cell marker; CD41b and CD62P, mostly originating from platelets; and CD9 and CD63, which also appeared to originate primarily from platelets) were significantly increased in smokers ($p = 0.000162$, $p = 0.000001$, $p = 0.000821$, $p = 0.000002$, and $p = 0.000248$, respectively; Figure 6c), despite no statistically significant difference in blood platelet concentration between smokers and non-smokers (Figure 6d). Conversely, median normalized MFI levels of CD1c, as well as T lymphocyte-derived CD8 and monocyte-derived CD14 markers on tetraspanin+ circulating EVs, were decreased in smokers ($p = 0.000535$, $p = 0.000227$, and $p = 0.00797$, respectively; Figure 6e), despite a significant increase in their blood leukocyte concentration ($p = 0.0001$, Figure 6f).

While neither sex nor age revealed any distinct patterns in PCA (Figure 6g,h), age affected the expression levels of CD146 and CD105 present on tetraspanin+ circulating EVs originating from endothelial cells (CD105 also from T lymphocytes; Figure 6i). Median normalized MFI levels of CD105 and CD146 markers on tetraspanin+ circulating EVs were significantly higher in the 18–29 years age group and 54–65 years age group, respectively, compared to the 30–44 years age group ($p = 0.000306$ and $p = 0.000332$, respectively). The difference was even more pronounced when analysing only males, indirectly suggesting the influence of sex on expression levels of CD146 and CD105 on tetraspanin+ circulating EVs (Figure 6j).

Altogether, while no global influence on expression of protein markers on tetraspanin+ circulating EVs was observed for any of the subject's factors, smoking and age were shown to contribute to inter-individual biological variation in levels of specific protein markers of platelets, leukocytes, or endothelial cells present on tetraspanin+ circulating EVs.

## 4 | Discussion

This study comprehensively quantified EVs with respect to cell origin in the plasma of a large cohort of healthy humans, to improve understanding of circulating EVs under physiological conditions, their biological variation, and sources of observed variation (Figure 7). Cell-specific circulating EV subsets exhibit a broad range of concentrations that do not correlate with cell-of-origin concentrations in blood, suggesting steady-state EV subset concentrations are regulated by complex mechanisms, which differ even for EV subsets from the same cell type. Interestingly, the tetraspanin+ subpopulation of circulating EVs largely originates from platelets and to a lesser extent from lymphocytes. We provide the first proof of high inter-individual biological variation of circulating EV subset concentrations in healthy humans, with differing levels of variation for EV subsets originating from the same cell type or with respect to its activation state. Tetraspanin+ circulating EVs show lower variation in expression levels of cell-type specific protein markers. Sex, menopausal status, age, and smoking contribute to inter-individual biological variation observed in concentrations of specific circulating EV subsets or specific protein marker expression levels on tetraspanin+ EVs, respectively. Nevertheless, no significant global effect of the subjects' factors on the circulating EVs or its tetraspanin+ subpopulation was identified.

Our results provide the first comprehensive, quantitative data towards the cell-origin atlas of the EV subsets in the plasma of healthy humans. Imaging flow cytometry analysis of plasma detected median EV concentration across all 25 studied subsets of $2.3 \times 10^7$/mL, which is in line with published flow cytometry studies on human circulating EVs (Johnsen et al. 2019; Bettin et al. 2022; Woud et al. 2022). Still, we observed up to a 221-fold variance in median concentrations among distinct EV subsets, with most numerous being EVs from activated platelets (GPIIb/IIIa*), followed by erythrocyte EVs (CD235a), activated granulocyte-derived EVs (CD66b), T lymphocyte EVs (CD152), EV released from APCs (HLA-DR), monocyte EVs (CD14), and activated endothelial EVs (CD90). Arraud et al. similarly observed with electron microscopy that 30% and 20% of circulating EVs were of platelet and erythrocyte origin, respectively (Arraud et al. 2014). In contrast, studies of the distribution of circulating EVs based on the RNA sequencing data underestimated the concentration of erythrocyte and neutrophil EVs and did not study endothelial EVs (Auber and Svenningsen 2022; Li et al. 2020). The abundance of the circulating EV subsets in our study does not reflect the abundance of their cells-of-origin, as measured by the complete blood count in the donor blood. For example, erythrocytes were 22 times more numerous than platelets but showed 3 times lower EV concentration if comparing GPIIb/IIIa*+ to CD235a+ EV subsets. This likely reflects the low EV secretion rate for erythrocytes compared to other blood cells (Auber and Svenningsen 2022; Gamonet et al. 2020) and/or the higher secretion rate of EVs from activated platelets (Guerreiro et al. 2024).

Still, we have evidence of further complexity to circulating EV subset steady-state concentration regulation, since correlation analysis detected no strong patterns among EV subsets originating from the same cell type. If we focus on EVs originating from activated platelets, they were the most numerous circulating EVs when measuring GPIIb/IIIa*+ EVs ($41.85 \times 10^6$/mL), and the least numerous when measuring CD62P+ EVs ($0.19 \times 10^6$/mL; also marker of activated endothelial cells). EV subsets carrying the general markers of platelets CD61 or CD41 had median concentrations of $2.03 \times 10^6$ and $3.44 \times 10^6$/mL, respectively. Importantly, large variation in platelet-circulating EV subset levels could reflect the diversity in the biogenesis of platelet EVs, which can be released by plasma membrane budding, extrusion of

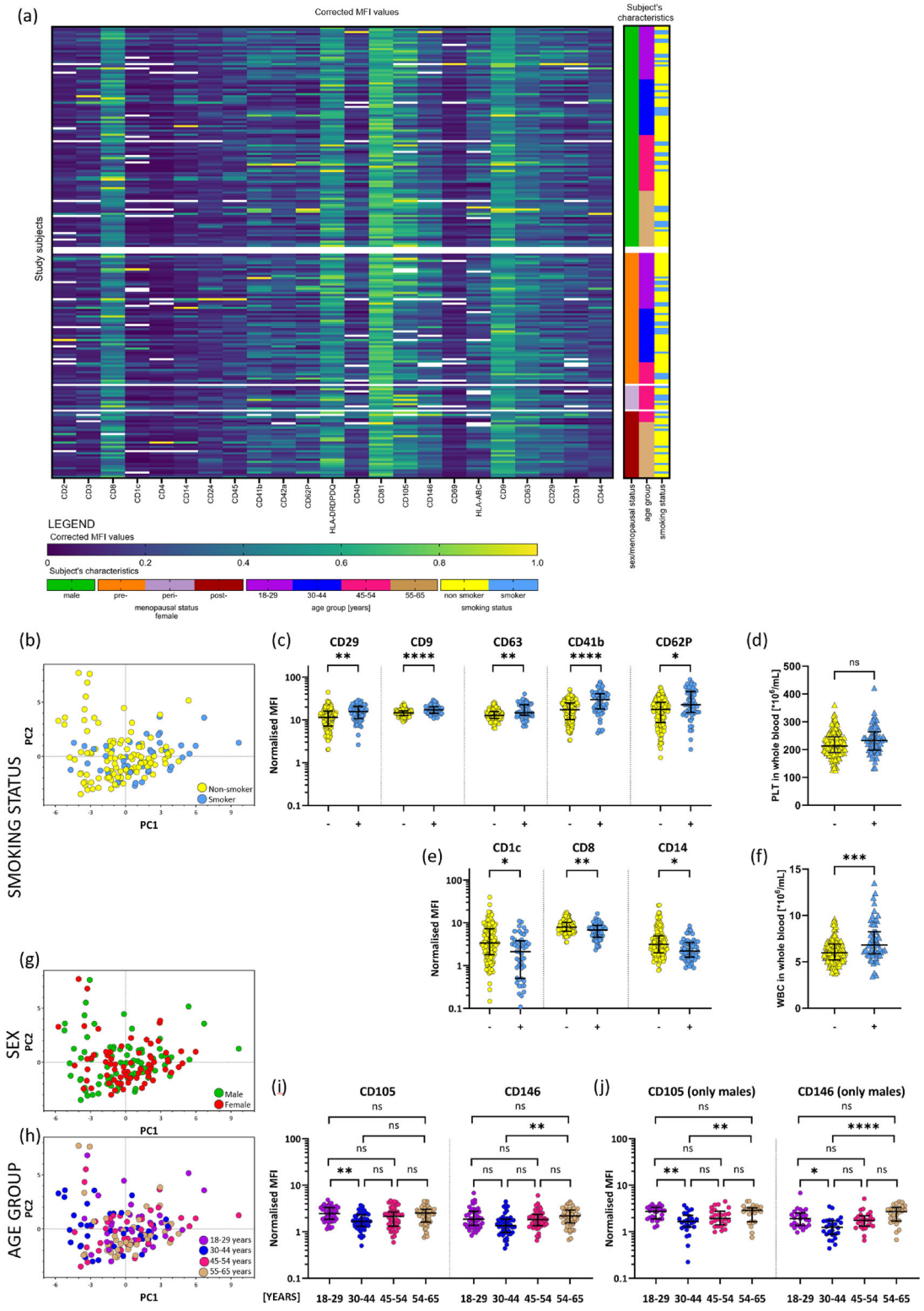


**FIGURE 6** | Sources of inter-individual biological variation observed in cell-type specific marker expression levels on tetraspanin+ circulating EVs. (a) Results of multiplex bead-based flow cytometry analysis of tetraspanin+ circulating EVs, corrected by dividing normalized MFIs by the largest measured normalized MFI value of each marker on tetraspanin+ circulating EVs. Each line represents one study subject. Subjects are arranged by their increasing age, sex, menopausal status, and smoking status. (b) PCA plot, coloured according to the smoking status of study subjects. Influence of smoking status on (c) expression levels of CD29+, CD9+, CD63+, CD41b+, and CD62P+ tetraspanin+ circulating EVs in plasma, and (d) platelet concentration in whole blood. PLT—platelets. Influence of smoking status on (e) expression levels of CD1c+, CD8+ and CD14+ tetraspanin+ circulating EVs in plasma, and (f) leukocyte concentration in whole blood. WBC—leukocytes. PCA plots, coloured according to (b) sex and (h) age group of study subjects. (i) Influence of age on expression levels of CD105+ and CD164+ tetraspanin+ circulating EVs. (j) Influence of age on expression levels of CD105+ and CD164+ tetraspanin+ circulating EVs presented only in man. Each dot represents one study subject. Black lines represent median with interquartile range; *—$p < 0.002$; **—$p < 0.0004$; ***—$p < 0.00004$; ****—$p < 0.000004$; ns—nonsignificant; MFI—median fluorescence intensity.

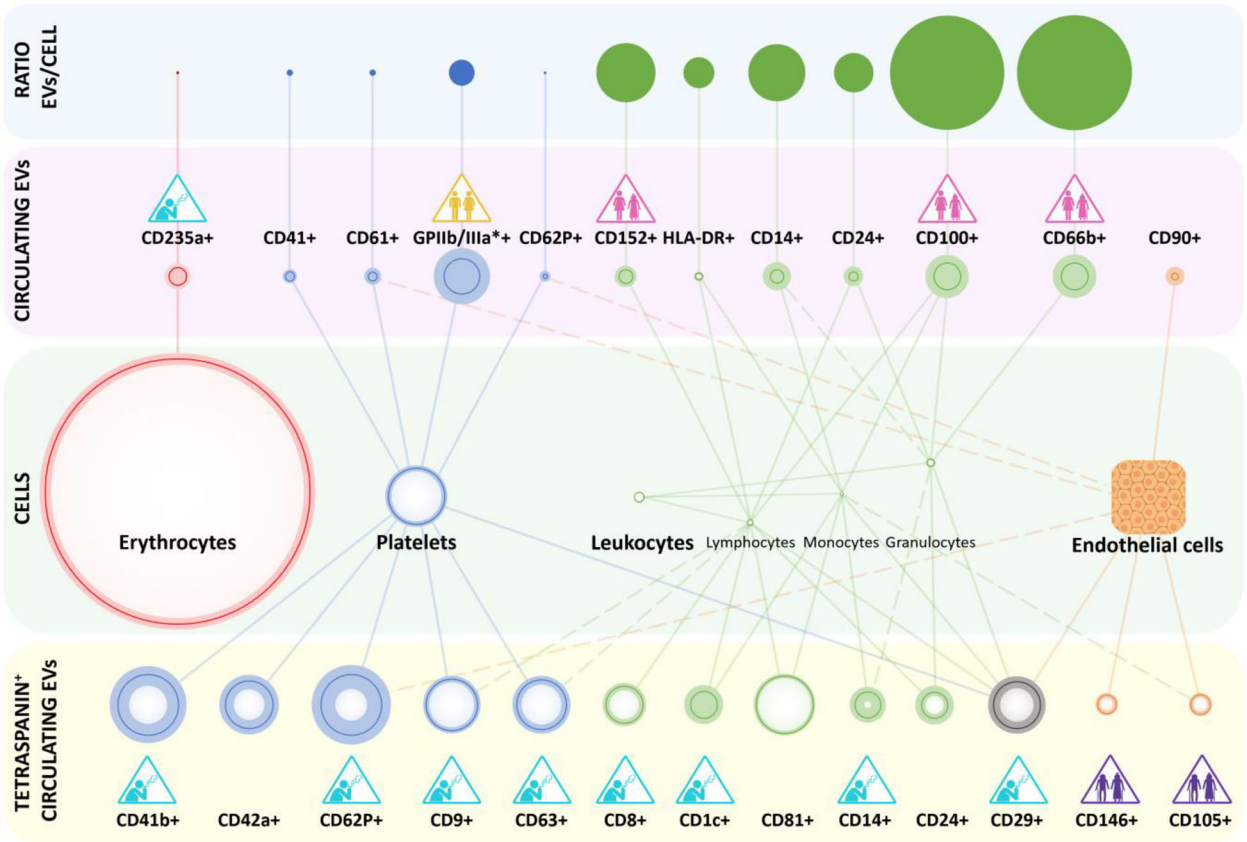


**FIGURE 7** | Schematic representation of circulating EVs in plasma of healthy humans: cellular origin and biological variation. Cell-specific circulating EV subsets show a wide range of concentrations as measured by imaging flow cytometry (pink field), which do not correspond to the concentrations of blood cells (green field). The sizes of the circles directly reflect the measured relative average concentrations of blood cells per mL of blood or EVs per mL of plasma, while the biological variation determined by the coefficient of variation (CV) is indicated by the shading of the circle borders. For endothelial cells, the size of the symbol does not reflect concentration as their count is unknown. Cellular sources of specific circulating EV subsets are indicated by a solid line from cells to EVs. When multiple cell types contribute to EVs, the primary cellular source is depicted with a solid line, while less common sources are shown with dashed lines. The estimated number of circulating EVs, carrying the indicated protein marker, per the cells-of-origin (blue field) suggests steady-state EV subset concentrations are regulated by complex mechanisms, which differ even for EV subsets from the same cell type. diverse patterns of EV subset release and/or uptake, even for EVs originating from the same cell type. The sizes of the full circles represent the relative ratio of EVs/cell. The EV-to-cell ratio for all EVs originating from any leukocytes is calculated as the number of EVs per leukocyte. The tetraspanin+ circulating EVs shows lower biological variation in expression levels of cell-type specific protein markers, as measured by the bead-based flow cytometry of enriched EVs (yellow field). The sizes of the circles represent the relative average normalized MFI signal for the indicated protein marker, while the biological variation (CV) is indicated by the shading of the circle borders. Cellular sources of specific circulating EV subsets are indicated by a solid line from cells to EVs. When multiple cell types contribute to EVs, the primary cellular source is depicted with a solid line, while less common sources are shown with dashed lines. We demonstrated a significant influence of sex (yellow icon), menopausal status (pink icon), age (violet icon), and smoking (blue icon) on inter-individual biological variation of specific circulating EV subsets and/or cell-type specific marker expression levels on tetraspanin+ EVs. For more detailed information, please refer to the manuscript. Image created by Biorender.com.

multivesicular $\alpha$-granules and cytoplasmic vacuoles, and plasma membrane blistering or "pearling" of platelets pseudopodia upon platelet activation (Heijnen et al. 1999; De Paoli et al. 2018). Further studies demonstrated that $Ca^{2+}$ triggers release of PS-exposing EVs from platelet plasma membrane, with lipid rafts playing an essential role (Wei, Malcor, and Harper 2018). Upon activation, the PS-exposing subpopulation of platelets expressed higher levels of CD62P and lower levels of activated GPIIb/IIIa* on their surface, compared to PS-negative platelets (Reddy et al. 2018), which could be replicated in the released EVs. PS exposure to the cell surface is recognized as one of the key 'eat me' signals for the clearance of apoptotic cells by macrophages (Segawa and Nagata 2015). In line with that, Matsumura et al. reported that circulating EVs not exposing PS on the membrane surface show slower clearance by macrophages in the mice blood (Matsumura et al. 2019). Accelerated clearance of PS+ EVs could thus explain the observed lower levels of the CD62P+ EV subset compared to the GPIIb/IIIa*+ EV subset in our cohort. Additionally, we cannot exclude megakaryocytes as the source of circulating EVs positive for CD41, CD42b, and PS, and negative for CD62P, since they were shown to release microparticles of submicron size from unbranched micropodia *in vitro* (Flaumenhaft et al. 2009; Gitz et al. 2014)(Stone et al. 2022). How this translates *in vivo* to circulating EVs in healthy adults is not fully understood but should be interpreted in the context of limited exposure of megakaryocytes to blood compared to platelets, which are

present in blood in high numbers (150–410 × $10^9$ /L). Interestingly, tetraspanin+ circulating EVs in healthy humans largely originated from platelets and showed a conserved pattern of protein marker expression across our study subjects, implying a similar mechanism of EV biogenesis. Among the three commonly used EV-related tetraspanins, only CD9 and CD63 seemed to be related to EVs of platelet origin, but not CD81.

We have shown high inter-individual biological variation of circulating EV subset concentrations in healthy humans, with the granulocyte-derived CD66b+ EVs, CD81+ EVs, activated endothelial CD90+ EVs, and CD44+ EVs contributing most to the observed variation, according to PCA. The median CV across all EV subsets was 162%, with the highest and the lowest CV of 719% and 63% observed for activated endothelial CD90+ EV and CD9+ EV subsets, respectively. For easier visualization, this translates to an almost 11,000-fold difference in CD90+ EV concentrations and only a 26-fold difference in CD9+EV concentrations among healthy individuals in our study. This variation surpasses even the high biological variation of commonly examined plasma analytes (Fest et al. 2018; Apoil et al. 2017) and underlines the necessity of establishing distinct reference intervals for each circulating EV subset intended for use as a biomarker, thus improving clinical decision-making. In comparison, tetraspanin+ circulating EVs exhibited lower variation in expression levels of cell-type-specific protein markers (median CV of 60%) but are not fully representative of the whole EV population in plasma, as they largely originate from platelets and, to a lesser extent, from lymphocytes. Of note, high inter-individual variation observed for some circulating EV subsets and expression of markers on tetraspanin+ EVs, including the CD90+ EVs and the CD4 marker, was due to high CVs observed in females (CV of 663% for CD90+ EVs and 127% for CD4 on tetraspanin+ EVs), supporting stratification of reference intervals by sex in such cases. Previous studies support the influence of female hormones on the blood CD90 concentrations and blood or endothelial cell surface expression of CD90 and CD4 (Bochev et al. 2022; Latorre et al. 2022; Elliott Williams et al. 2023). For example, increased concentrations of soluble CD90 are linked to endometriosis (Bochev et al. 2022) and the fluctuations in oestrogen and progesterone levels during the menstrual cycle and pregnancy influence the activity and regulation of CD4+ T cells (Polese et al. 2014). Interestingly, even EV subsets originating from the same cell type showed differing levels of biological variation. In the case of platelet EVs, CD41+, GPIIb/IIIa*+, and CD62P+ EV (also marker of activated endothelial cells) subsets had CVs of 138%, 153%, and 637%, respectively. This could suggest the preferred use of CD41+ and GPIIb/IIIa*+ EVs as markers of platelets and activated platelets in plasma as they are more consistent across healthy humans, but on the other hand, CD62P+ EV subsets might be richer in information regarding ongoing (pato)physiological processes. Further studies are needed to better understand the biological variation of circulating EVs and how it is affected by disease.

The comprehensive association analysis and PCA performed here support the hypothesis that sex, menopausal status, age, and smoking contribute to inter-individual biological variation observed in circulating EVs in healthy humans, but the influence was limited to specific EV subsets and/or cell-type specific marker expression levels on tetraspanin+ EVs. This is supported by the studies in which age, sex, and/or smoking status were shown to affect specific circulating EV subsets (Enjeti et al. 2017; Gustafson et al. 2015) and protein profiles on tetraspanin+ circulating EVs (Bæk, Varming, and Jørgensen 2016). In contrast, Eitan et al. implied the global effects of age on circulating EV concentration, but this might be due to the detection of all precipitated nanoparticles from plasma, not just EVs, with NTA in their study (Eitan et al. 2017). Specifically, our study found higher concentrations of GPIIb/IIIa*+ platelet-derived EVs in females, indicating a sex-related pro-coagulant profile, consistent with reports of elevated platelet (CD62P, CD41, CD42a)-derived microvesicles in female (Gustafson et al. 2015). Furthermore, the pro-coagulative nature of microvesicles was higher during the luteal phase of the menstrual cycle, compared to the follicular phase (Toth, Nikolajek, and Rank 2007), implicating the involvement of female sex hormones in this phenomenon. Here, smoking also influenced platelet-derived EVs, as smokers showed increased expression of CD41b and CD62P on tetraspanin+ circulating EVs, supporting previous findings by Mobarrez et al. that smoking even a single cigarette is reflected in elevated microparticles from platelets (Mobarrez et al. 2014). Additionally, smokers showed significantly lower levels of erythrocyte-derived CD235a+ circulating EVs in our study, aligning with findings of increased macrocytic erythrocytes in smokers, since smoking affects the morphology of the red blood cells (Aldosari et al. 2020). This could similarly cause perturbation of vesiculation from erythrocytes in our cohort. Interestingly, pre-menopausal females had significantly higher concentrations of leukocyte-derived CD100+, CD152+, and CD66b+ EVs than post-menopausal females. While immune variations occur in menopause, differences in immune cell-derived circulating EVs have not been reported previously. Others have shown decreases in microvesicles from erythrocytes (CD235a+) and endothelial cells (CD105+) in post-menopausal females (Gustafson et al. 2015; Enjeti et al. 2017), which was not reflected in our cohort. On the other hand, smoking reduced T lymphocytic CD8+ and monocytic CD14+ EVs in our study, supporting the modulatory effect of cigarette smoke on immune cells (Russell et al. 2022). Analysing endothelial cell-derived EVs, we observed a significant decrease in CD146+ EVs in early middle-aged adults compared to older adults, a novel finding as CD146's role in ageing has not been described before. We also noted a decrease in CD105+ EVs in early middle-aged adults compared to young adults, while Enjeti et al. reported a continuous decrease in CD105+ microvesicles across age groups (Enjeti et al. 2017).

Our study is the first to demonstrate high biological inter-individual variation in circulating EVs across healthy humans, which can be partly explained by the influence of sex, menopausal status, age, and smoking on specific blood cells and endothelial cells. Still, several limitations of our study should be acknowledged. Our healthy human cohort was composed of Slovenian blood donors of South Slavic ethnicity, limiting exploration of the influence of race on circulating EVs. Furthermore, study subjects were not fasted, since eating a non-fatty meal before blood donation is a routine recommendation. However, statistical analysis found no influence of serum lipoprotein and insulin values on the study results. Although relying on self-reported data on smoking, exercise, height, and weight can introduce potential biases, we minimized those by performing in-person interviews conducted by the same medical doctor, rather than through self-administered questionnaires. Additionally, ours was a single

time-point (cross-sectional) study, limiting our understanding of biological intra-individual variation of circulating EVs over time. Still, we employed strict inclusion criteria, so the study cohort represents apparently healthy adult population, and have performed comprehensive quality checks and reporting (MIBlood-EV, MIFlowCyte-EV) to ensure consistency and minimize the influence of pre-analytical variables and technical variation on the study outcomes. We acknowledge that the reported concentrations of EV subsets are specific to the imaging flow cytometer used in our study, as detection limits for fluorescence and size depend on the instrument's configuration.

Still, our study is the first to comprehensively quantify circulating EVs with respect to cell origin in plasma of a large cohort of healthy humans. It improves the understanding of the circulating EV subsets under physiological conditions, their biological variation, and sources of observed variation. Our findings have important implications for fundamental research and clinical applications of plasma EVs, especially as biomarkers of diverse diseases.

### Author Contributions

**Marija Holcar**: conceptualization (lead), data curation (lead), formal analysis (lead), investigation (lead), methodology (lead), resources (lead), visualization (lead), writing–original draft (lead), writing–review and editing (lead). **Ivica Marić**: conceptualization (lead), data curation (lead), funding acquisition (supporting), investigation (lead), methodology (lead), resources (lead), writing–review and editing (lead), **Tobias Tertel**: formal analysis (supporting), investigation (lead), methodology (supporting), resources (supporting), writing–review and editing (supporting). **Katja Goričar**: formal analysis (supporting), investigation (supporting), methodology (supporting), resources (supporting), writing–review and editing (supporting). **Urška Čegovnik Primožič**: formal analysis (supporting), investigation (supporting), methodology (supporting), writing–review and editing (supporting). **Darko Černe**: methodology (supporting), resources (supporting), writing–review and editing (supporting). **Bernd Giebel**: methodology (supporting), resources (supporting), writing–review and editing (supporting). **Metka Lenassi**: conceptualization (lead), funding acquisition (lead), project administration (lead), resources (lead), supervision (lead), writing–original draft (lead), writing–review and editing (lead).


### Acknowledgements

The authors would like to thank Nina Mavec for her help with the enrichment of EVs from plasma.


### Conflicts of Interest

The authors report no conflicts of interest.

### References


Akoglu, H. 2018. "User's Guide to Correlation Coefficients." *Turkish Journal of Emergency Medicine* 18, no. 3: 91–93. https://doi.org/10.1016/j.tjem.2018.08.001.

Aldosari, K. H., G. Ahmad, S. Al-Ghamdi, et al. 2020. "The Influence and Impact of Smoking on Red Blood Cell Morphology and Buccal Microflora : A Case-Control Study." *Journal of Clinical Laboratory Analysis* 34, no. 6: 3–7. https://doi.org/10.1002/jcla.23212.

Apoil, P. A., B. Puissant-Lubrano, N. Congy-Jolivet, et al. 2017. "Reference Values for T, B and NK Human Lymphocyte Subpopulations in Adults." *Data in Brief* 12: 400–404. https://doi.org/10.1016/j.dib.2017.04.019.

Arraud, N., R. Linares, S. Tan, et al. 2014. "Extracellular Vesicles From Blood Plasma: Determination of Their Morphology, Size, Phenotype and Concentration." *Journal of Thrombosis and Haemostasis* 12, no. 5: 614–627. https://doi.org/10.1111/jth.12554.

Auber, M., and P. Svenningsen. 2022. "An Estimate of Extracellular Vesicle Secretion Rates of Human Blood Cells." *Journal of Extracellular Biology* 1, no. 6: e46. https://doi.org/10.1002/jex2.46.

Aziz, N., R. Detels, J. J. Quint, D. Gjertson, T. Ryner, and A. W. Butch. 2019. "Biological Variation of Immunological Blood Biomarkers in Healthy Individuals and Quality Goals for Biomarker Tests." *BMC Immunology* 20, no. 1: 1–11. https://doi.org/10.1186/s12865-019-0313-0.

Bæk, R., K. Varming, and M. M. Jørgensen. 2016. "Does Smoking, Age or Gender Affect the Protein Phenotype of Extracellular Vesicles in Plasma?" *Transfusion and Apheresis Science* 55, no. 1: 44–52. https://doi.org/10.1016/j.transci.2016.07.012.

Beetler, D. J., D. N. Di Florio, K. A. Bruno, et al. 2023. "Extracellular Vesicles as Personalized Medicine." *Molecular Aspects of Medicine* 91: 101155. https://doi.org/10.1016/j.mam.2022.101155.

Berckmans, R. J., R. Lacroix, C. M. Hau, A. Sturk, and R. Nieuwland. 2019. "Extracellular Vesicles and Coagulation in Blood From Healthy Humans Revisited." *Journal of Extracellular Vesicles* 8, no. 1: 1688936. https://doi.org/10.1080/20013078.2019.1688936.

Bettin, B., A. Gasecka, B. O. Li, et al. 2022. "Removal of Platelets From Blood Plasma to Improve the Quality of Extracellular Vesicle Research." *Journal of Thrombosis and Haemostasis* 20, no. 11: 2679–2685. https://doi.org/10.1111/jth.15867.

Bochev, I. M., I. I. Karagyozov, N. M. Magunska, et al. 2022. "Evaluation of Soluble CD90: Potential for Diagnostic Significance in Endometriosis Patients." *Disease Markers* 2022, no. 1: 9345858. https://doi.org/10.1155/2022/9345858.

Brahmer, A., E. Neuberger, L. Esch-Heisser, et al. 2019. "Platelets, Endothelial Cells and Leukocytes Contribute to the Exercise-Triggered Release of Extracellular Vesicles Into the Circulation." *Journal of Extracellular Vesicles* 8, no. 1: 1–19. https://doi.org/10.1080/20013078.2019.1615820.

"CD Marker Handbook Human and Mouse". 2016. Becton, Dickinson and Company. https://www.bdbiosciences.com/documents/cd_marker_handbook.pdf.

Driedonks, T., L. Jiang, B. Carlson, et al. 2022. "Pharmacokinetics and Biodistribution of Extracellular Vesicles Administered Intravenously and Intranasally to Macaca Nemestrina." *Journal of Extracellular Biology* 1, no. 10: 1–33. https://doi.org/10.1002/jex2.59.

EDQM. 2023. *Guide to the Preparation, Use and Quality Assurance of Blood Components. Transfusion Medicine*. Strasbourg, France: European Directorate for the Quality of Medicines & HealthCare.

Eitan, E., J. Green, M. Bodogai, et al. 2017. "Age-Related Changes in Plasma Extracellular Vesicle Characteristics and Internalization by Leukocytes." *Scientific Reports* 7, no. 1: 1–14. https://doi.org/10.1038/s41598-017-01386-z.

Elliott Williams, M., F. P. Hardnett, A. N. Sheth, et al. 2023. "The Menstrual Cycle Regulates Migratory CD4 T-Cell Surveillance in the Female Reproductive Tract via CCR5 Signaling." *Mucosal Immunology* 17, no. 1: 41–53. https://doi.org/10.1016/j.mucimm.2023.10.002.

Enjeti, A. K., A. Ariyarajah, A. D'Crus, M. Seldon, and L. F. Lincz. 2017. "Circulating Microvesicle Number, Function and Small RNA Content Vary With Age, Gender, Smoking Status, Lipid and Hormone Profiles." *Thrombosis Research* 156: 65–72. https://doi.org/10.1016/j.thromres.2017.04.019.

Fest, J., R. Ruiter, M. Arfan Ikram, T. Voortman, C. H. J. V. Eijck, and B. H. Stricker. 2018. "Reference Values for White Blood-Cell-Based Inflammatory Markers in the Rotterdam Study: A Population-Based Prospective Cohort Study." *Scientific Reports* 8, no. 1: 1–7. https://doi.org/10.1038/s41598-018-28646-w.

Flaumenhaft, R., J. R. Dilks, J. Richardson, et al. 2009. "Megakaryocyte-Derived Microparticles: Direct Visualization and Distinction From Platelet-Derived Microparticles." *Blood* 113, no. 5: 1112–1121. https://doi.org/10.1182/blood-2008-06-163832.

Gamonet, C., M. Desmarets, G. Mourey, et al. 2020. "Processing Methods and Storage Duration Impact Extracellular Vesicle Counts in Red Blood Cell Units." *Blood Advances* 4, no. 21: 5527–5539. https://doi.org/10.1182/bloodadvances.2020001658.

Gitz, E., A. Y. Pollitt, J. J. Gitz-Francois, et al. 2014. "CLEC-2 Expression Is Maintained on Activated Platelets and on Platelet Microparticles." *Blood* 124, no. 14: 2262–2270. https://doi.org/10.1182/blood-2014-05-572818.

Görgens, A., M. Bremer, R. Ferrer-Tur, et al. 2019. "Optimisation of Imaging Flow Cytometry for the Analysis of Single Extracellular Vesicles by Using Fluorescence-Tagged Vesicles as Biological Reference Material." *Journal of Extracellular Vesicles* 8, no. 1: 1–25. https://doi.org/10.1080/20013078.2019.1587567.

Grant, D., N. Wanner, M. Frimel, Serpil Erzurum, and K. Asosingh. 2021. "Comprehensive Phenotyping of Endothelial Cells Using Flow Cytometry 2: Human." *Cytometry Part A* 99, no. 3: 257–264. https://doi.org/10.1002/cyto.a.24293.

Guerreiro, E. M., S. G. Kruglik, S. Swamy, et al. 2024. "Extracellular Vesicles From Activated Platelets Possess a Phospholipid-Rich Biomolecular Profile and Enhance Prothrombinase Activity." *Journal of Thrombosis and Haemostasis* 22, no. 5. 1463–1474. https://doi.org/10.1016/j.jtha.2024.01.004.

Gustafson, C. M., A. J. Shepherd, V. M. Miller, and M. Jayachandran. 2015. "Age- and Sex-Specific Differences in Blood-Borne Microvesicles From Apparently Healthy Humans." *Biology of Sex Differences* 6, no. 1:. https://doi.org/10.1186/s13293-015-0028-8.

Han, V., K. Serrano, and D. V. Devine. 2010. "A Comparative Study of Common Techniques Used to Measure Haemolysis in Stored Red Cell Concentrates." *Vox Sanguinis* 98, no. 2: 116–123. https://doi.org/10.1111/j.1423-0410.2009.01249.x.

Heijnen, H. F. G., A. E. Schiel, R. Fijnheer, H. J. Geuze, and J. J. Sixma. 1999. "Activated Platelets Release Two Types of Membrane Vesicles: Microvesicles by Surface Shedding and Exosomes Derived From Exocytosis of Multivesicular Bodies and α-Granules." *Blood* 94, no. 11: 3791–3799. https://doi.org/10.1182/blood.v94.11.3791.

Holcar, M., J. Ferdin, S. Sitar, et al. 2020. "Enrichment of Plasma Extracellular Vesicles for Reliable Quantification of Their Size and Concentration for Biomarker Discovery." *Scientific Reports* 10, no. 1: 1–13. https://doi.org/10.1038/s41598-020-78422-y.

Jakše, B., U. Godnov, and S. Pinter. 2022. "Nutritional Status of Slovene Adults in the Post-COVID-19 Epidemic Period." *European Journal of Investigation in Health, Psychology and Education* 12, no. 12: 1729–1742. https://doi.org/10.3390/ejihpe12120122.

Johnsen, K. B., J. M. Gudbergsson, T. L. Andresen, and J. B. Simonsen. 2019. "What Is the Blood Concentration of Extracellular Vesicles? Implications for the Use of Extracellular Vesicles as Blood-Borne Biomarkers of Cancer." *Biochimica Et Biophysica Acta—Reviews on Cancer* 1871, no. 1: 109–116. https://doi.org/10.1016/j.bbcan.2018.11.006.

Kalina, T., K. Fišer, M. Pérez-Andrés, et al. 2019. "CD Maps—Dynamic Profiling of CD1–CD100 Surface Expression on Human Leukocyte and Lymphocyte Subsets." *Frontiers in Immunology* 10: 2434. https://doi.org/10.3389/fimmu.2019.02434.

Kumar, M. A., S. K. Baba, H. Q. Sadida, et al. 2024. "Extracellular vesicles as tools and targets in therapy for diseases." *Sig Transduct Target Ther* 9, no. 27: 1–41. https://doi.org/10.1038/s41392-024-01735-1.

Körbling, M., and P. Anderlini. 2001. "Peripheral Blood Stem Cell versus Bone Marrow Allotransplantation: Does the Source of Hematopoietic Stem Cells Matter?" *Blood* 98, no. 10: 2900–2908. https://doi.org/10.1182/blood.V98.10.2900.

Lacroix, R., C. Judicone, P. Poncelet, et al. 2012. "Impact of Pre-Analytical Parameters on the Measurement of Circulating Microparticles: Towards Standardization of Protocol." *Journal of Thrombosis and Haemostasis* 10, no. 3: 437–446. https://doi.org/10.1111/j.1538-7836.2011.04610.x.

Latorre, M. C., C. Gómez-Oro, I. Olivera-Valle, et al. 2022. "Vaginal Neutrophil Infiltration Is Contingent on Ovarian Cycle Phase and Independent of Pathogen Infection." *Frontiers in Immunology* 13: 1031941. https://doi.org/10.3389/fimmu.2022.1031941.

Li, Y. Y., X. He, Q. Li, et al. 2020. "EV-Origin: Enumerating the Tissue-Cellular Origin of Circulating Extracellular Vesicles Using ExLR Profile." *Computational and Structural Biotechnology Journal* 18: 2851–2859. https://doi.org/10.1016/j.csbj.2020.10.002.

Loconte, L., D. Arguedas, R. El, et al. 2023. "Detection of the Interactions of Tumour Derived Extracellular Vesicles With Immune Cells Is Dependent on EV-Labelling Methods." *Journal of Extracellular Vesicles* 12, no. 12: e12384. https://doi.org/10.1002/jev2.12384.

Matsumoto, A., Y. Takahashi, K. Ogata, et al. 2021. "Phosphatidylserine-Deficient Small Extracellular Vesicle Is a Major Somatic Cell-Derived SEV Subpopulation in Blood." *Iscience* 24, no. 8: 102839. https://doi.org/10.1016/j.isci.2021.102839.

Matsumura, S., T. Minamisawa, K. Suga, et al. 2019. "Subtypes of Tumour Cell-Derived Small Extracellular Vesicles Having Differently Externalized Phosphatidylserine." *Journal of Extracellular Vesicles* 8, no. 1: 1579541. https://doi.org/10.1080/20013078.2019.1579541.

Mobarrez, F., L. Antoniewicz, J. A. Bosson, J. Kuhl, D. S. Pisetsky, and M. Lundbäck. 2014. "The Effects of Smoking on Levels of Endothelial Progenitor Cells and Microparticles in the Blood of Healthy Volunteers." *PLoS ONE* 9, no. 2: e90314. https://doi.org/10.1371/journal.pone.0090314.

Mosbach, M. L., C. Pfafenrot, E. P. von Strandmann, A. Bindereif, and C. Preußer. 2021. "Molecular Determinants for RNA Release Into Extracellular Vesicles." *Cells* 10, no. 10: 2674. https://doi.org/10.3390/cells10102674.

Muraoka, S., M. Hirano, J. Isoyama, S. Nagayama, T. Tomonaga, and J. Adachi. 2022. "Comprehensive Proteomic Profiling of Plasma and Serum Phosphatidylserine-Positive Extracellular Vesicles Reveals Tissue-Specific Proteins." *Iscience* 25, no. 4: 104012. https://doi.org/10.1016/j.isci.2022.104012.

Nieuwland, R., and P. R. M. Siljander. 2024. "A Beginner's Guide to Study Extracellular Vesicles in Human Blood Plasma and Serum." *Journal of Extracellular Vesicles* 13, no. 1: e12400. https://doi.org/10.1002/jev2.12400.

de Oliveira, G. P., J. A. Welsh, and B. Pinckney. 2023. "Human Red Blood Cells Release Microvesicles With Distinct Sizes and Protein Composition That Alter Neutrophil Phagocytosis." *Journal of Extracellular Biology* 2, no. 11: e107. https://doi.org/10.1002/jex2.107.

Ozarda, Y., V. Higgins, and K. Adeli. 2019. "Verification of Reference Intervals in Routine Clinical Laboratories: Practical Challenges and Recommendations." *Clinical Chemistry and Laboratory Medicine* 57, no. 1: 30–37. https://doi.org/10.1515/cclm-2018-0059.

de Paoli, S. H., T. Z. Tegegn, O. K. Elhelu, et al. 2018. "Dissecting the Biochemical Architecture and Morphological Release Pathways of the Human Platelet Extracellular Vesiculome." *Cellular and Molecular Life Sciences* 75, no. 20: 3781–3801. https://doi.org/10.1007/s00018-018-2771-6.

Polese, B., V. Gridelet, E. Araklioti, H. Martens, S. Perrier, and V. Geenen. 2014. "The Endocrine Milieu and CD4 T-Lymphocyte Polarization During Pregnancy." *Frontiers in Endocrinology* 5: 106. https://doi.org/10.3389/fendo.2014.00106.

Rai, A., K. Huynh, Q. I. Hui Poh, et al. 2024. "Multi-Omics Discovery of Hallmark Protein and Lipid Features of Circulating Small Extracellular Vesicles in Humans." *BioRxiv*. March 7, 2024. https://doi.org/10.1101/2024.03.16.585131.

Reddy, E. C., H. Wang, H. Christensen, et al. 2018. "Analysis of Procoagulant Phosphatidylserine-Exposing Platelets by Imaging Flow Cytometry." *Research and Practice in Thrombosis and Haemostasis* 2, no. 4: 736–750. https://doi.org/10.1002/rth2.12144.

Royo, F., C. Théry, J. M. Falcón-Pérez, R. Nieuwland, and K. W. Witwer. 2020. "Methods for Separation and Characterization of Extracellular Vesicles: Results of a Worldwide Survey Performed by the ISEV Rigor and Standardization Subcommittee." *Cells* 9, no. 9: 1955. https://doi.org/10.3390/cells9091955.

Russell, A. E., Z. Liao, M. Tkach, et al. 2022. "Cigarette Smoke-Induced Extracellular Vesicles From Dendritic Cells Alter T-Cell Activation and HIV Replication." *Toxicology Letters* 360: 33–43. https://doi.org/10.1016/j.toxlet.2022.02.004.

Segawa, K., and S. Nagata. 2015. "An Apoptotic 'Eat Me' Signal: Phosphatidylserine Exposure." *Trends in Cell Biology* 25, no. 11: 639–650. https://doi.org/10.1016/j.tcb.2015.08.003.

Spurgeon, B. E. J., and A. L. Frelinger. 2022. "Comprehensive Phenotyping of Human Platelets by Single-Cell Cytometry." *Cytometry Part A* 101, no. 4: 290–297. https://doi.org/10.1002/cyto.a.24531.

Stone, A. P., E. Nikols, D. Freire, and K. R. Machlus. 2022. "The Pathobiology of Platelet and Megakaryocyte Extracellular Vesicles: A (C)Lot Has Changed." *Journal of Thrombosis and Haemostasis* 20, no. 7: 1550–1558. https://doi.org/10.1111/jth.15750.

Tertel, T., M. Bremer, C. Maire, et al. 2020. "High-Resolution Imaging Flow Cytometry Reveals Impact of Incubation Temperature on Labeling of Extracellular Vesicles With Antibodies." *Cytometry Part A* 97, no. 6: 602–609. https://doi.org/10.1002/cyto.a.24034.

Tertel, T., A. Görgens, and B. Giebel. 2020. "Analysis of Individual Extracellular Vesicles by Imaging Flow Cytometry." *Methods in Enzymology* 645: 55–78. https://doi.org/10.1016/bs.mie.2020.05.013.

Tosar, J. P., K. Witwer, and A. Cayota. 2021. "Revisiting Extracellular RNA Release, Processing, and Function." *Trends in Biochemical Sciences* 46, no. 6: 438–445. https://doi.org/10.1016/j.tibs.2020.12.008.

Toth, B., K. Nikolajek, A. Rank, et al. 2007. "Gender-Specific and Menstrual Cycle Dependent Differences in Circulating Microparticles." *Platelets* 18, no. 7: 515–521. https://doi.org/10.1080/09537100701525843.

Troussard, X., S. Vol, E. Cornet, et al. 2014. "Full Blood Count Normal Reference Values for Adults in France." *Journal of Clinical Pathology* 67, no. 4: 341–344. https://doi.org/10.1136/jclinpath-2013-201687.

Vallejo, M. C., S. Sarkar, E. C. Elliott, et al. 2023. "A Proteomic Meta-Analysis Refinement of Plasma Extracellular Vesicles." *Scientific Data* 10, no. 1: 1–14. https://doi.org/10.1038/s41597-023-02748-1.

Van Pelt L., S. K. Joost, T. Hwandih, et al. 2022. "Reference Intervals for Sysmex XN Hematological Parameters as Assessed in the Dutch Lifelines Cohort." *Clinical Chemistry and Laboratory Medicine* 60, no. 6: 907–920. https://doi.org/10.1515/cclm-2022-0094.

Wandel, E., A. Saalbach, D. Sittig, C. Gebhardt, and G. Aust. 2012. "Thy-1 (CD90) Is an Interacting Partner for CD97 on Activated Endothelial Cells." *Journal of Immunology* 188, no. 3: 1442–1450. https://doi.org/10.4049/jimmunol.1003944.

Wei, H., J. D. M. Malcor, and M. T. Harper. 2018. "Lipid Rafts Are Essential for Release of Phosphatidylserine-Exposing Extracellular Vesicles From Platelets." *Scientific Reports* 8, no. 1: 1–11. https://doi.org/10.1038/s41598-018-28363-4.

Welsh, J. A., E. van der Pol, B. A. Bettin, et al. 2020. "Towards Defining Reference Materials for Measuring Extracellular Vesicle Refractive Index, Epitope Abundance, Size and Concentration." *Journal of Extracellular Vesicles* 9, no. 1816641: 1–17. https://doi.org/10.1080/20013078.2020.1816641.

Widjaja, A., R. J. Morris, J. C. Levy, et al. 1999. "Within- and Between-Subject Variation in Commonly Measured Anthropometric and Biochemical Variables." *Clinical Chemistry* 45, no. 4: 561–566. https://doi.org/10.1093/clinchem/45.4.561.

Woud, W. W., E. van der Pol, E. Mul, et al. 2022. "An Imaging Flow Cytometry-Based Methodology for the Analysis of Single Extracellular Vesicles in Unprocessed Human Plasma." *Communications Biology* 5, no. 1: 1–14. https://doi.org/10.1038/s42003-022-03569-5.

**Supporting Information**

Additional supporting information can be found online in the Supporting Information section.